Aus dem Institut für Landwirtschaftliche Verfahrenstechnik der
Christian-Albrechts-Universität zu Kiel

DRY MASS ESTIMATION AT LINEAR FOREST OBJECTS VIA STRUCTURE FROM MOTION

Dissertation zur Erlangung des Doktorgrades der Agrar- und
Ernährungswissenschaftlichen Fakultät der
Christian-Albrechts-Universität zu Kiel

vorgelegt von

Stefan Lingner

aus Iserlohn

Kiel 2018

Dekan: Prof. Dr. Dr. Henning
1. Berichterstatter: Prof. Dr. Eberhart Hartung
2. Berichterstatter: Prof. Dr. Tim Diekötter
Tag der mündlichen Prüfung: 23.01.2019

Gedruckt mit Genehmigung der Agrar- und Ernährungswissenschaftlichen Fakultät

Contents

1 General Introduction

Already Julius Caesar (*13 July 100 BC) mentioned hedge banks in the area of today's Germany in his Bellum Gallicum (Pott, 1989). He described hedge banks as living thorn hedges whose density was maintained by downward bent young shoots. In the 18th century when most of the hedge banks in Schleswig-Holstein were created the picture was still the same. Small walls of stones and soil were build. On these walls shrubs and trees were planted. Young shoots of these shrubs and trees were bent down to increase the hedges' density. These living fences had multiple benefits. These fences enclosed parcels, protected crop from cattle and provided wood. They sheltered cattle from snow and wind in winter and provided shade in summer. Hedge banks still serve as windbreak to reduce wind erosion and to improve micro-climate for adjacent crops (Kort, 1988; Nuberg, 1998). In the 19th century a large number of hedge banks was annihilated. Larger parcels were preferred due to more efficient farming techniques. In 1935 a first law was enacted for hedge bank protection. Today hedge banks in Schleswig-Holstein are a protected habitat according to § 21 State Conservation Act of Schleswig-Holstein (LNatSchG) with reference to § 30 Federal Nature Conservation Act (BNatSchG). Today there are around 46,000 km of hedge banks left in Schleswig-Holstein.

Hedge banks as field margins are an important factor for faunal and floral biodiversity in agricultural landscapes (Marshall, 2002, 2004). They serve as habitat and migration path for numerous species. Field margins increase the biodiversity of invertebrates (Lagerl et al., 1992; Duelli and Obrist, 2003), birds (Vickery and Fuller, 1999; Sparks et al., 1996; Vickery et al., 2009) and mammals (Verboom and Huitema, 1997; Kotzageorgis and Mason, 2009; Tattersall et al., 2002). Additionally hedge banks serve as migration path for diverse species (Gaywood, 1993; Burel, 1989). To preserve this ecological value the hedge banks need to be artificially maintained (Roßkamp, 2001; Ministerium für Energiewende, Landwirtschaft, Umwelt und ländliche Räume des Landes Schleswig-Holstein, 2017). This maintenance mainly consists of full cutting back in intervals of 10 to 15 years with only a few trees left standing. This cutting back allows shrubs to prevail, which in turn serve as shelter and breeding ground for numerous animals.

According to the European Renewable Energy Directive (2009/28/EG) renewable energy is supposed to cover at least 20 % of the gross energy consumption in 2020 within the European Union. In Germany, the amount of woody biomass used as a source for energy has already increased during the last decades (Mantau, 2012). The future demand for woody biomass could in part be supplied by harvested wood of existing hedge banks and roadside plantings (Isensee et al., 2000; Seidel et al., 2015).

Ideal would be the local usage of sustainable hedge bank wood chips while the ecological value of the hedge banks is maintained. Some farmers in Schleswig-Holstein already have a wood chips heating plant. For hedge bank management and harvesting logistic it is impotent to estimate the potential wood yield of a hedge bank before

harvesting. However, the wood yield of hedge banks is very diverse and hard to estimate in advance. To date no reliable and time efficient (non-destructive) method exists to estimate the potential woody biomass of hedge banks.

The aim of the current thesis was to develop and to test a technique for biomass estimation at linear forest objects. At first the literature was searched for different methods of woody biomass estimation. At second different methods were tested at linear forest objects in Schleswig-Holstein and the results were compared to reference dry masses.

Chapter 2 presents the literature review of biomass estimation at various different spatial scales. This chapter reports the state of the art of different methods for non-invasive tree mass estimation techniques. Different studies about biomass estimations at different spatial scales were compared based on three assessment criterias: accuracy, efficiency, and technical requirements.

Chapter 3 compares two methods of wood yield estimation at hedge banks. Test objects were three hedge banks in Schleswig-Holstein. The first method is an estimation based on allometric equation via diameter at breast height (DBH). The second method is an estimation based on structure from motion (SfM). The results of both methods were compared to results of the (invasive) reference method: weighing after harvesting.

Chapter 4 compares two methods of wood yield estimation at eleven linear forest objects. Test objects were five hedge banks and six roadside plantings in Schleswig-Holstein. The first method is an estimation based on aerial images plus age of object. Like in Chapter 3 the second method is an estimation based on SfM. The results of both methods were compared to results of the (invasive) reference method: weighing after harvesting.

Chapter 5 addresses multiple questions that arose during the process of the previous papers. The topics investigated further in this chapter are: Analysis of sensitivity (seasonal effect, amount of images, resolution of images), SfM vs. experienced person, temporal pattern of growth and ecological value vs. dry mass yield.

The general discussion covers experiences gained, decisions made and recommendations for the future that are worth to be discussed generally for all previous chapters.

References

F. Burel. Landscape structure effects on carabid beetles spatial patterns in western France. *Landscape Ecology*, 2(4):215–226, June 1989. ISSN 0921-2973, 1572-9761. doi: 10.1007/BF00125092. URL `http://link.springer.com/10.1007/BF00125092`.

P. Duelli and M. K. Obrist. Regional biodiversity in an agricultural landscape: the contribution of seminatural habitat islands. *Basic and Applied Ecology*, 4 (2):129–138, Jan. 2003. ISSN 14391791. doi: 10.1078/1439-1791-00140. URL `http://linkinghub.elsevier.com/retrieve/pii/S1439179104701085`.

M. Gaywood. *Linear features: linear habitats and wildlife corridors*, volume 60 of *English Nature Research Reports*. University of Southampton, Southampton, 1993.

E. Isensee, D. K. Stübig, and C. Lubkowitz. Bergung und Aufbereitung von Knick- und Schwachholz. *Landtechnik–Agricultural Engineering*, 55(5):346–347, 2000.

J. Kort. Benefits of Windbreaks to Field and Forage Crops. *Agriculture, Ecosystems and Environment*, 22(23):165–190, 1988.

G. C. Kotzageorgis and C. F. Mason. Small mammal populations in relation to hedgerow structure in an arable landscape. *Journal of Zoology*, 242(3):425–434, Mar. 2009. ISSN 09528369. doi: 10.1111/j.1469-7998.1997.tb03846.x. URL `http://doi.wiley.com/10.1111/j.1469-7998.1997.tb03846.x`.

J. Lagerl, J. Stark, and B. Svensson. Margins of agricultural fields as habitats for pollinating insects. *Agriculture, Ecosystems and Environment*, 40:117–124, 1992.

U. Mantau. *Holzrohstoffbilanz Deutschland, Entwicklungen und Szenarien des Holzaufkommens und der Holzverwendung 1987 bis 2015*. PhD thesis, Universität Hamburg, Hamburg, 2012.

E. Marshall. Introducing field margin ecology in Europe. *Agriculture, Ecosystems & Environment*, 89(1-2):1–4, Apr. 2002. ISSN 01678809. doi: 10.1016/S0167-8809(01)00314-0.

E. J. P. Marshall. Agricultural landscapes: field margin habitats and their interaction with crop production. *Journal of Crop Improvement*, 12(1-2):365–404, 2004.

Ministerium für Energiewende, Landwirtschaft, Umwelt und ländliche Räume des Landes Schleswig-Holstein. Durchführungsbestimmungen zum Knickschutz, Jan. 2017.

I. Nuberg. Effect of shelter on temperate crops: a review to define research for Australian conditions. *Agroforestry Systems*, 41:3–34, 1998.

R. Pott. Historische und aktuelle Formen der Bewirtschaftung von Hecken in Nordwestdeutschland. *Forstwissenschaftliches Centralblatt*, 108(1):111–121, Dec. 1989. ISSN 1439-0337. doi: 10.1007/BF02741400. URL https://doi.org/10.1007/BF02741400.

T. Roßkamp. Zur Bestandssituation der Hecken in Niedersachsen und deren Auswirkung auf die Vogelwelt, dargestellt an traditionellen Wallheckenlandschaften im nordwestlichen Niedersachsen. *Seevögel - Zeitschrift Verein Jordsand,*, 22(2), 2001.

D. Seidel, G. Busch, B. Krause, C. Bade, C. Fessel, and C. Kleinn. Quantification of Biomass Production Potentials from Trees Outside Forests – A Case Study from Central Germany. *BioEnergy Research*, 8(3):1344–1351, Sept. 2015. ISSN 1939-1234, 1939-1242. doi: 10.1007/s12155-015-9596-z. URL http://link.springer.com/10.1007/s12155-015-9596-z.

T. Sparks, T. Parish, and S. Hinsley. Breeding birds in field boundaries in an agricultural landscape. *Agriculture, Ecosystems & Environment*, 60(1):1–8, Nov. 1996. ISSN 01678809. doi: 10.1016/S0167-8809(96)01067-5. URL http://linkinghub.elsevier.com/retrieve/pii/S0167880996010675.

F. H. Tattersall, D. W. Macdonald, B. J. Hart, P. Johnson, W. Manley, and R. Feber. Is habitat linearity important for small mammal communities on farmland?: Effect of habitat linearity on small mammals. *Journal of Applied Ecology*, 39(4):643–652, Aug. 2002. ISSN 00218901, 13652664. doi: 10.1046/j.1365-2664.2002.00741.x. URL http://doi.wiley.com/10.1046/j.1365-2664.2002.00741.x.

B. Verboom and H. Huitema. The importance of linear landscape elements for the pipistrelle *Pipistrellus pipistrellus* and the serotine bat *Eptesicus serotinus*. *Landscape Ecology*, 12(2):117–125, Apr. 1997. ISSN 0921-2973, 1572-9761. doi: 10.1007/BF02698211. URL http://link.springer.com/10.1007/BF02698211.

J. Vickery and R. Fuller. *Use of cereal fields by birds: a review in relation to field margin managements*. BTO Research Report No. 195. BTO, National Centre for Ornithology, Thetford, Norfolk, 1999. ISBN 978-1-902576-08-4. OCLC: 183082939.

J. A. Vickery, R. E. Feber, and R. J. Fuller. Arable field margins managed for biodiversity conservation: A review of food resource provision for farmland birds. *Agriculture, Ecosystems & Environment*, 133(1-2):1–13, Sept. 2009. ISSN 01678809. doi: 10.1016/j.agee.2009.05.012. URL http://linkinghub.elsevier.com/retrieve/pii/S0167880909001625.

2 Applicability of different non-invasive methods for tree mass estimation: a review

Stefan Lingner, Eiko Thiessen, Eberhard Hartung

published in *Forest Ecology and Management* 398 (2017) 208–215

2.1 Abstract

Biomass estimations of trees are used at various different spatial scales. Along with the scale, there are diverse demands on accuracy and technical requirements. This paper reports the state of the art of different methods for non-invasive tree mass estimation techniques. Different studies about biomass estimations at different spatial scales were compared on basis of three assessment criteria: accuracy, efficiency, and technical requirements. Publications were searched via Google Scholar, Web of Science and ScienceDirect including years from 1980 to 2016. References of 20 studies could be used to compare 10 methods of biomass estimation.

Allometric approaches are comparably accurate but are suitable for small area applications only. Remote sensing techniques are less accurate but more efficient. Lidar and SfM appear to be the most efficient and most accurate techniques for medium sized area applications. Especially SfM applications are promising due to lower technical requirements. Optical images are suitable for coarse but large area applications.

2.2 Introduction

There are various reasons for the demand of accurate non-invasive tree mass estimations. On a larger spatial scale, accurate mass estimates are important for climate change modelling studies, greenhouse gas inventories and terrestrial carbon accounting (Muukkonen and Heiskanen, 2005). On a smaller spatial scale, accurate mass estimations are made on ecological and commercial purposes (Miller et al., 2015). Consequently, a vast number of studies presents approaches to estimate the mass of entire forests or single trees (Muukkonen, 2007; Tiwari and Singh, 1984; Véga et al., 2015). The current study reviews the most common techniques for tree mass estimation at different scales.

The exact measurement of a tree's mass requires destructive/invasive methods like felling and weighing. However, these destructive methods are expensive, time consuming and not appropriate for all objectives, like in ecological studies. Consequently, more efficient and less or non-invasive but less accurate methods are applied. These tree mass estimation procedures are always a trade-off between accuracy and efficiency. The need to find an appropriate trade-off for any specific objective appears to be the major reason for the large number of different methods.

Tree mass can be seen as commercially valid stem mass or as biomass in general which includes small branches and foliage. The majority of the reviewed studies are aiming to predict total above ground biomass (Dandois and Ellis, 2010; Popescu, 2007). Other studies like Yu et al. (2013) are aiming to estimate stem mass only and studies like Kankare et al. (2013) have estimated both.

The aim of this study is to present an overview of available techniques for non-invasive tree mass estimation. Techniques are compared based on accuracy, efficiency, and technical requirements.

2.3 Methods

Study selection

Publications regarding methods for tree mass estimation were searched via Google Scholar, Web of Science and ScienceDirect including years from 1980 to 2016. The following key words were used in different combinations: “tree”, “forest”, “biomass”, “mass” and “estimation”. Altogether, about 100 publications were sighted, but only a total of 20 publications were suitable for comparison. These studies were used to review 10 different methods for tree mass estimation.

Assessment criteria

Altogether three assessment criteria were used to compare the different methods:

- accuracy,
- efficiency,
- and technical requirements.

Accuracy

The absolute root mean square error (RMSE) or relative root mean square error (rRMSE) were the accuracy estimates used by reviewed studies throughout different methods. Consequently, the rRMSE was chosen for accuracy comparison. If no rRMSE but absolute RMSE was reported in a particular study, the rRMSE was estimated based on absolute RMSE and the approximate mean mass value $\overline{y}$ (Equation 2.1). If values of multiple publications regarding the same method could be processed a mean rRMSE was calculated.

$$rRMSE = \frac{\sqrt{\frac{1}{n}\sum_{i=1}^{n}(y_i - \hat{y}_i)^2}}{\overline{y}} \tag{2.1}$$

Nevertheless, the comparison of different studies based on the rRMSE should be done with caution. Only about 30 % of all reviewed studies have actually used destructive weighing to gain exact reference values. The majority of the reviewed studies have used reference values that were merely estimated. The current review outlines the way reference values were obtained when presenting a study.

Efficiency

Comparing monitored plot sizes in hectare (ha) assesses the spatial efficiency of the different methods. This assessment bases on the underlying assumption that more efficient methods and less efficient methods were used to monitor larger plot sizes and smaller plot sizes, respectively.

Technical requirements

Technical requirements are listed to get an idea about technical effort and costs for applying the reviewed methods. For final comparison, these technical requirements were broadly divided into four categories: very low, low, high and very high.

2.4 Results and Discussion

Allometric equations

Various studies have presented allometric regressions to estimate biomass from non-invasive measurements like DBH (Diameter at Breast Height) or height (Brown et al., 1989; Ketterings et al., 2001; Nelson et al., 1999). However, appropriate regression coefficients for these allometric equations vary between sites and species (Ketterings et al., 2001; Komiyama et al., 2008; Telenius and Verwijst, 1995). Thus, finding appropriate coefficients is the general challenge in these approaches. This problem is usually either solved by destructive sampling or the use of literature values. Another option is the use of adaptive equations like presented in Ketterings et al. (2001). However, the technical requirement for these methods is low, which is basically a measuring tape.

Segura et al. (2006) yielded an rRMSE of 13 % by estimating biomass of four different shade tree species (for coffee plants) based on diameter. Reference values in this study were gained by weighing. Annighöfer et al. (2016) have estimated biomass of seedlings and saplings of various European tree species. Using height and root-collar-diameter as predicting variables resulted in a mean RMSE of 462 g. The mean weight of a sample was around 5000 g, this results in an rRMSE of 9 %. Reference values in this study were gained by weighing as well.

Despite its challenges, allometric approaches appear to be still the most established method in small area applications (Alves et al., 1997; Brown et al., 1989; Muukkonen, 2007). One of the major reasons for its spread is likely to be the low grade of technical requirements. However, their application is very time consuming at larger spatial scales. Table 2.1 presents studies using allometric equations for biomass estimation.

Optical images

The processing of optical images appears to be an appropriate method for large area but coarse biomass estimations of homogeneous stands (Muukkonen and Heiskanen, 2007; Tokola and Heikkilä, 1997; Tomppo et al., 2002). Optical images consist of pixels including information of passively remote sensed visible and infrared wavelengths (Goetz et al., 1985). The green band can either be directly correlated with biomass or the bands are first transferred into vegetation indices and afterwards correlated with biomass (Muukkonen and Heiskanen, 2005). Large area optical images can be obtained via airplane and satellite. Technical requirements for optical images based studies are basically these images, which can be made autonomously using a hired aircraft or alternatively directly bought from service providers.

Muukkonen and Heiskanen (2005) have investigated the correlation between bands registered by an ASTER satellite and stand volume listed in stand wise inventory

Table 2.1: Studies estimating biomass using allometric equations. Studies in bold could be used for rRMSE comparison. Their rRMSE-values are listed in Table 2.6

Author	Object	Biomass reference data
Schmitt and Grigal (1981)	Birches in US and Canada	Meta-study using data sets of 9 original studies
Uhl et al. (1988)	Tropical forest, Brazil	Destructive sampling of 8–16 individuals per species
Brown et al. (1989)	Tropical forest, Brazil and Venezuela	Meta-study using data sets of 9 original studies
Overman et al. (1994)	Tropical forest, Colombia	Destructive sampling of 54 trees
Telenius and Verwijst (1995)	Willow in short rotation forest, Sweden	Destructive sampling of 10 shoots per stand
Alves et al. (1997)	Tropical forest, Brazil	No reference measurements
Nelson et al. (1999)	Tropical forest, Brazil	Destructive sampling of 17–27 individuals per species
Ketterings et al. (2001)	Tropical forest, Indonesia	Destructive sampling of 29 trees
Komiyama et al. (2005)	Mangrove species, South-East Asia	Destructive sampling of 104 individuals of 10 species
Segura et al. (2006)	**Shade trees (for coffee plants), Nicaragua**	**Destructive sampling of 34 individuals of 4 species**
Wang (2006)	Temperate forest, China	Destructive sampling of 100 individuals of 10 species
Muukkonen and Heiskanen (2007)	7 European tree species	Psoudoobservations generated by equations from literature
Annighöfer et al. (2016)	**Seedlings and saplings of European tree species**	**Weighing of 4468 individuals of 19 species**

data. This stand wise inventory data were provided by the Ministry of Agriculture and Forestry and the Finnish Forest Research Institute. It can be assumed that stand volume in these inventory data sets is not measured but estimated. Regression models including multiple bands (red and near-infrared) for predicting tree biomass lead to an rRMSE of 40 %. In the study of Muukkonen and Heiskanen (2005) the forests' sizes ranged between 0.006 and 30 ha. ASTER satellite images have a pixel size of 15 m. The same authors have used the same models on MODIS satellite data with a pixel size of 250 m to predict tree biomass of forests with sizes up to 2,000,000 ha (Muukkonen and Heiskanen, 2007). The biomass estimation in this study had an rRMSE of 8 %. Ploton et al. (2012) have estimated biomass by processing Google Earth images. Biomass estimations based on allometric equations in plot sizes of 1 ha were used as reference data. The rRMSE in this study was 14 %.

Optical images cover large areas, but are suitable for homogeneous stands only and are not applicable in mountain regions (Sader et al., 1989). Consequently, analysis based on optical images are appropriate to a limited extend only for commercial forestry applications. Table 2.2 presents studies using optical images for biomass estimation.

Radar

Synthetic Aperture Radar (SAR) is an active remote sensing technique, sending a pulse of microwave radiation and calculating distances based on interferometry (Mitchard et al., 2009; Toan et al., 2004). Radar approaches for biomass estimations are suitable for large areas but achieve the best accuracies only at sparse or regrowing forests with little biomass (Kasischke et al., 1997; Toan et al., 2004). Airplane based Radar approaches (Hyde et al., 2007; Mette et al., 2004), as well as satellite based Radar approaches (Ranson et al., 1995; Toan et al., 2004), have been applied to predict forest biomass.

Hyde et al. (2007) have used an airplane based RaStudies in bolddar to estimate biomass. Reference values in this study were estimated by allometric equations based on manually measured DBH in plots with sizes of 0.1225 ha. The rRMSE for predicting biomass with Radar-derived values was at 51 %. However, using both Lidar and Radar derived values for predicting biomass decreased the rRMSE to approximately 24 %. The essential technical instrument for equivalent applications is an aircraft equipped with a downward looking Radar.

The satellite based Radar approach to estimate forest biomass from Ranson et al. (1995) yielded an rRMSE of 17 %. Allometric equations of sample trees in reference plots were used for reference values. The satellite based Radar approach from Englhart et al. (2011) yielded an rRMSE of approximately 50 %. Airborne Lidar was used to estimate reference biomass in 1 ha plots.

Radar based methods appear to be efficient for biomass estimations on a large area scale. However, the large wavelengths of a Radar are disadvantageous compared to a laser in Lidar based methods. The larger the wavelength the harder it is to reconstruct small objects. Consequently, the Radar based method is suitable for homogeneous stands only. Table 2.3 presents studies using Radar for biomass estimation.

Table 2.2: Studies estimating biomass using optical images. Studies in bold could be used for rRMSE comparison. Their rRMSE-values are listed in Table 2.6. [1]This paper presents an incorrect rRMSE equation. However, it is assumed that the correct equation is used for rRMSE calculation.

Author	Object	Method	Biomass reference data
Poso et al. (1987)	Boreal forest, Finland	Satellite	Estimations based on relascope measurements
Sader et al. (1989)	Tropical forest, Puerto Rico	Satellite	Allometric equation in 72 1 ha plots
Sader et al. (1989)	Warm temperate forest, US	Satellite	Allometric equation in 44 plots
Roy and Ravan (1996)	Dry deciduous forests, India	Satellite	Allometric equation in 18 0.1 ha plots
Hyyppä (2000)	Boreal forest, Finland	Satellite/Airplane	Estimations based on relascope measurements of 40 stands
Tomppo et al. (2002)	Boreal forest, Finland	Satellite	Estimated forest inventory data
Jong et al. (2003)	Mediterranean oak forest, France	Airplane	Allometric equation in 83 0.1 ha plots
Muukkonen and Heiskanen (2005)	**Boreal forest, Finland**	**Satellite**	**Estimated forest inventory data**
Muukkonen and Heiskanen (2007)[1]	**Boreal forest, Finland**	**Satellite**	**Estimated forest inventory data**
Ploton et al. (2012)	**Tropical forest, India**	**Satellite**	**Allometric equation in 15 1 ha plots**
Seidel et al. (2015)	Trees outside forests, Germany	Airplane	No reference data

Table 2.3: Studies estimating biomass using Radar. Studies in bold could be used for rRMSE comparison. Their rRMSE-values are listed in Table 2.6

Author	Object	Method	Biomass reference data
Hussin et al. (1991)	Mixed forest, US	Airborne	Estimated forest inventory data
Le Toan et al. (1991)	Pine dominated forest, France	Airborne	Estimated forest inventory data
Dobson et al. (1992)	Pine forest, France	Airborne	Allometric equation of sample trees
Rauste et a. (1994)	Conifer forest, Germany	Airborne	Estimated forest inventory data
Rignot et al. (1994)	Boreal forest, Alaska	Airborne	Allometric equation of 3150 trees in 21 plots
Ranson et al. (1995)	**Boreal Forest, Canada**	**Spaceborne**	**Allometric equation in 21 stands**
Hyyppä (2000)	Boreal Forest, Finland	Airborne	Estimations based on relascope measurements of 40 stands
Milne et al. (2000)	Woodland, Australia	Airborne and Spaceborne	Allometric equation of sample trees in 99 plots
Mette et al. (2004)	Conifer forest, Germany	Airborne	Estimated forest inventory data
Mitchard et al. (2009)	Tropical savannas and woodlands in Africa	Spaceborne	Allometric equation in 253 plots
Hyde et al. (2007)	**Pine dominated forest, US**	**Airborne**	**Allometric equation in 49 0.1 ha plots**
Englhart et al. (2011)	**Tropical forest, Indonesia**	**Spaceborne**	**Airborne Lidar estimated data**

Lidar

Lidar is an active remote sensing technology that measures the time of light traveling form a sensor to a target and consequently calculates the distance (Dubayah and Drake, 2000; Lim et al., 2003; Pfeifer et al., 2015). The major advantage of Lidar-systems compared to systems operating with optical images is the possibility to obtain and process multiple returns per pulse. The pulse of a Lidar ideally is not only returned from canopy but as well from vegetation underneath and from ground (Lim et al., 2003). From this information, the vegetation structure can be derived, which enables biomass estimation. For tree parameter estimation terrestrial (Dassot et al., 2012; Kankare et al., 2013; Raumonen et al., 2015), airborne (Hyyppä et al., 2001; Lin et al., 2011; Popescu, 2007), and spaceborne (Lefsky et al., 2005; Popescu et al., 2011) approaches have been applied.

Kankare et al. (2013) have used terrestrial laser scanning to estimate biomass of single trees. Destructive weighing yielded reference biomass values in this study. Individual linear multivariate models for two species of conifers were conducted to predict reference biomass with Lidar data. These models yielded an rRMSE of 13 % for Scots pines (*Pinus sylvestris*) and an rRMSE of 12 % for Norway spruces (*Picea abies*). Yu et al. (2013) achieved an rRMSE of 13 % for the same two species. Reference values in this study came from destructive measurements. Yao et al. (2011) have used a terrestrial near-infrared Lidar to derive forest parameters like biomass in a hardwood and conifer forest in Australia. These biomass estimates were compared to reference estimates based on allometric equations. The linear model yielded an rRMSE of approximately 11 %. Calders et al. (2015) estimated the biomass of eucalyptus trees in Australia and achieved an rRMSE of 16 %. The essential technical instrument for equivalent applications is a terrestrial laser scanner.

Airborne applications have been airplane based (Hyde et al., 2007; Hyyppä et al., 2001; Popescu, 2007) or unmanned aerial vehicle (UAV) based (Lin et al., 2011; Wallace et al., 2012).

Lidar derived DBH estimates were used to predict biomass in the airplane based study of Popescu (2007). These biomass estimates were compared to reference estimates estimated by allometric equations based on manually measured DBH. This study yielded an rRMSE of 47 %. Plot sizes in this study were 0.04 ha and a cross-hatch flight pattern resulted in 2.6 laser points per m^2 in average. In the airplane based study of Hyde et al. (2007) Lidar derived height estimates were used to predict biomass. Like in Popescu (2007) biomass estimates were compared to reference estimates estimated by allometric equations based on manually measured DBH. However, Hyde et al. (2007) yielded an rRMSE of approximately 26 %. Plot sizes in this study were 0.1225 ha. Véga et al. (2015) achieved an rRMSE of 7 % when comparing allometric biomass estimates with Lidar derived biomass estimates. The essential technical instrument for equivalent applications is an aircraft equipped with a Lidar sensor. Alternatively, these data can be bought from service providers.

Lin et al. (2011) and Wallace et al. (2012) have used UAV based Lidar-systems to estimate forest parameters. Unfortunately, they did not present biomass estimations. However, other estimations like tree height appear to be more accurate than in airplane based approaches due to higher point densities (Lin et al., 2011). Based on this comparison the rRMSE is assumed to be around 20 %. For UAV based Lidar

applications it is essential to have a Lidar sensor plus an UAV that is not only capable of carrying that lidar sensor but also is equipped with a GPS unit or another positioning system accurate enough to meet the requirements for a Lidar based point cloud generation.

Lefsky et al. (2005) and Popescu et al. (2011) have used satellite based Lidar to estimate biomass. Lefsky et al. (2005) have compared their spaceborne height estimates with estimated biomass reference values. Allometric equations based on manually measured DBH were used to yield these biomass reference estimates. A linear model comparing both estimates had an rRMSE of approximately 39 %. Popescu et al. (2011) have compared their spaceborne tree height estimates with biomass estimates retrieved by airborne Lidar and yielded an rRMSE of approximately 25 %. Technical requirements for equivalent studies are basically spaceborne Lidar data, which are obtained via service providers like NASA.

For large area applications, the remote sensing technique Lidar appears to be the most common technique (Dubayah and Drake, 2000; Hyyppä et al., 2001; Kankare et al., 2013). The air or spaceborne techniques cover large areas and the accuracy appears to be adequate. However, the application of a terrestrial Lidar that is used on a smaller spatial scale is likely to be very time consuming. The measurements have to be done from various positions. Table 2.4 presents studies using Lidar for biomass estimation.

Structure from Motion

Structure from Motion (SfM) is a remote sensing technique that constructs 3D point clouds from numerous overlapping photos. The underlying algorithms use methods of computer vision and photogrammetry. These algorithms are looking for key points in individual photos and are matching these points with associated key points in other photos. Thus, the camera position and its calibration plus the location of the key points are estimated. For tree parameter estimation top-down approaches (Dandois and Ellis, 2010; Fritz et al., 2013; Zarco-Tejada et al., 2014) and side-on approaches (Miller et al., 2015) have been applied.

The aircraft based top-down SfM approach by Dandois and Ellis (2010) have been applied to 0.0625 ha sized plots. In this study, biomass reference values per study plot were estimated by allometric equations based on a manually measured DBH. SfM estimated biomass was modeled versus these reference values. The linear model yielded an rRMSE of 54 %. The essential technical instrument for equivalent approaches is a camera-equipped aircraft.

The side-on SfM approach by Miller et al. (2015) has been applied to single trees. Biomass was not estimated in this study but total tree volume. Reference volume values were determined by water displacement of the entire tree. The linear model to predict reference volume with SfM estimated volume yielded an rRMSE of 19 %. The technical requirement in this study was a low-cost and hand-held camera only.

SfM appears to be less often applied for biomass estimation of trees than Lidar. However, progress in computing power and SfM algorithms lately focuses attention on SfM for forest parameter estimation (Fritz et al., 2013; Miller et al., 2015). The major disadvantage of Lidar versus SfM appears to be its high costs (Tao et al., 2011). In contrast to a Lidar-UAV, a SfM-UAV needs a regular GPS receiver plus a digital

Table 2.4: Studies estimating biomass using Lidar. Studies in bold could be used for rRMSE comparison. Their rRMSE-values are listed in Table 2.6. [1]This paper presents an incorrect rRMSE equation. However, it is assumed that the correct equation is used for rRMSE calculation.

Author	Object	Method	Biomass reference data
Hyyppä et al. (2001)	Boreal forest, Finland	Airborne	Estimated forest inventory data
Lefsky et al. (2002)	Diverse forests, US and Canada	Airborne	Allometric equations
Lefsky et al. (2005)	**Tropical forest, Brazil; temperate forest, US**	**Spaceborne**	**Allometric equations in 19 plots**
Hyde et al. (2007)	**Pine dominated forest, US**	**Airborne**	**Allometric equation of sample trees in 49 plots**
Popescu et al. (2007)	**Pine forest, US**	**Airborne**	**Allometric equation of 43 sample trees**
Li et al. (2011)	Mixed forest, Finland	UAV	No reference data
Popescu et al. (2011)	**Mixed forest, US**	**Spaceborne**	**Allometric equation of 1004 trees in 62 plots**
Yao et al. (2011)	**Hardwood and conifer forest, Australia**	**Terrestrial**	**Allometric equation in 1 ha reference plots**
Dassot et al. (2012)	Single trees, France	Terrestrial	Destructive measurements of 42 trees
Wallace et al. (2012)	Single trees, Australia	UAV	No reference data
Kankare et al. (2013)[1]	**Single trees, Finland**	**Terrestrial**	**Destructive measurements of 63 trees**
Yu et al. (2013)	**Single trees, Finland**	**Terrestrial**	**Destructive measurements of 30 trees**
Calders et al. (2015)	**Single eucalyptus trees, Australia**	**Terrestrial**	**Destructive measurements of 65 trees**
Hackenberg et al. (2015)	Single trees	Terrestrial	Destructive measurements
Raumonen et al. (2015)	Oaks, England; Eucalyptus trees, Australia	Terrestrial	Allometric equations
Véga et al. (2015)	**Tropic forest, India**	**Airborne**	**Allometric equation in 15 1 ha plots**

camera only. Nex and Remondino (2014) presents the UAV state of the art and give an overview of different platform types.

Fritz et al. (2013) have compared point clouds of trees generated by Lidar and SfM. The point clouds generated by Lidar were a lot denser than those generated by SfM, which lead to a more detailed model. However, in this study, a side-on Lidar approach was compared to a top-down SfM approach. Pole shaped objects like trees are generally harder to grasp from above than from the side. In contrast to Fritz et al. (2013), the studies from Baltsavias et al. (2008) and Leberl et al. (2010) found, that point clouds generated by SfM are at least as dense as those generated by Lidar. However, densities of point clouds mainly depend on the setup applied. At SfM applications point densities always depend on camera resolution, distance to object and computing effort. While at Lidar applications densities depend on frequency, spacing, and distance. Table 2.5 presents studies using SfM for biomass estimation.

2.5 Conclusion

Studies with presented or calculable rRMSE are presented in Table 2.6 for comparison. Out of these values, the author calculated mean values per method. Figure 2.1 presents these mean values versus the efficiency based on plot sizes used in the publications. Table 2.7 presents a classification of the technical requirements and suitable forest conditions per method.

The rRMSE values in Table 2.6 have to be compared with caution. As mentioned above reference values were generated in different ways. Destructive weighing is the only method to gain accurate values, and then only, if the sample size and sample selection were adequate. Consequently, a publication that has used destructive weighing to get reference values is likely to be more accurate than a method that has used estimated reference values but achieved the same or lower rRMSE. For example, methods based on optical images yielded rRMSE values in the range of the rRMSE values of lidar based methods. However, the papers presenting the lidar methods used more accurate sampling methods to gain reference values. In this case, a direct comparison of rRMSE values would be misleading.

The essence of the current study is: Allometric approaches are comparably accurate, but time consuming. Consequently, they are suitable for small area applications only. Lidar and SfM appear to be the most efficient and most accurate techniques for medium sized area applications. Especially SfM applications are promising due to lower technical requirements. Optical images are suitable for coarse but large area applications.

Table 2.5: Selection of studies estimating biomass using SfM. Studies in bold could be used for rRMSE comparison. Their rRMSE-values are listed in Table 2.6

Author	Object	Method	Biomass reference data
Dandois and Ellis (2010)	**Mixed forest, US**	**Top-down**	**Allometric equation**
Fritz et al. (2013)	Oak dominated forest, Germany	Top-down	DBH measurement with terrestrial Lidar
Zarco-Tejada et al. (2014)	Olive orchard, Spain	Top-down	Manually measured height of 152 trees
Miller et al. (2015)	**Individual trees, New Zealand**	**Side-on**	**Water displacement of 30 individual trees**

Table 2.6: Overview of reviewed papers. [1]This paper presents an incorrect RMSE/rRMSE equation. However, it is assumed that the correct equation is used for RMSE/rRMSE calculation

Method	Reference Data	rRMSE	Author
Allometric equations	Destructive sampling 34 individuals of 4 species	13	Segura et al. (2006)
Allometric equations	Weighing of 4468 individuals of 19 species	9	Annighöfer et al. (2016)
Spaceborne Optical Images	Estimated forest inventory data	40	Muukkonen and Heiskanen (2005)
Spaceborne Optical Images	Estimated forest inventory data	8[1]	Muukkonen and Heiskanen (2007)
Spaceborne Optical Images	Allometric equation in 15 1 ha plots	14	Ploton et al. (2012)
Airborne Radar	Allometric equation of in 49 0.1 ha plots	51	Hyde et al. (2007)
Spaceborne Radar	Allometric equation of in 21 stands	17	Ranson et al. (1995)
Spaceborne Radar	Airborne Lidar estimated data	50	Englhart et al. (2011)
Terrestrial Lidar	Allometric equation in 1 ha plots	11	Yao et al. (2011)
Terrestrial Lidar	Destructive measurements of 63 trees	13[1]	Kankare et al. (2013)
Terrestrial Lidar	Destructive measurements of 30 trees	13	Yu et al. (2013)
Terrestrial Lidar	Destructive measurements of 65 trees	16	Calders et al. (2015)
Airborne Lidar	Allometric equation in 49 0.1 ha plots	26	Hyde et al. (2007)
Airborne Lidar	Allometric equation of 43 trees	47	Popescu (2007)
Airborne Lidar	Allometric equation in 15 1 ha plots	7	Véga et al. (2015)
UAV Lidar	No biomass estimation	20	Lin et al. (2011) and Wallace et al. (2012)
Spaceborne Lidar	Allometric equations in 19 plots	39	Lefsky et al. (2005)
Spaceborne Lidar	Allometric equation of 1004 trees in 62 plots	25	Popescu (2011)
SfM top-down	Allometric equations	54	Dandois and Ellis (2010)
SfM side-on	Water displacement	19	Miller et al. (2015)

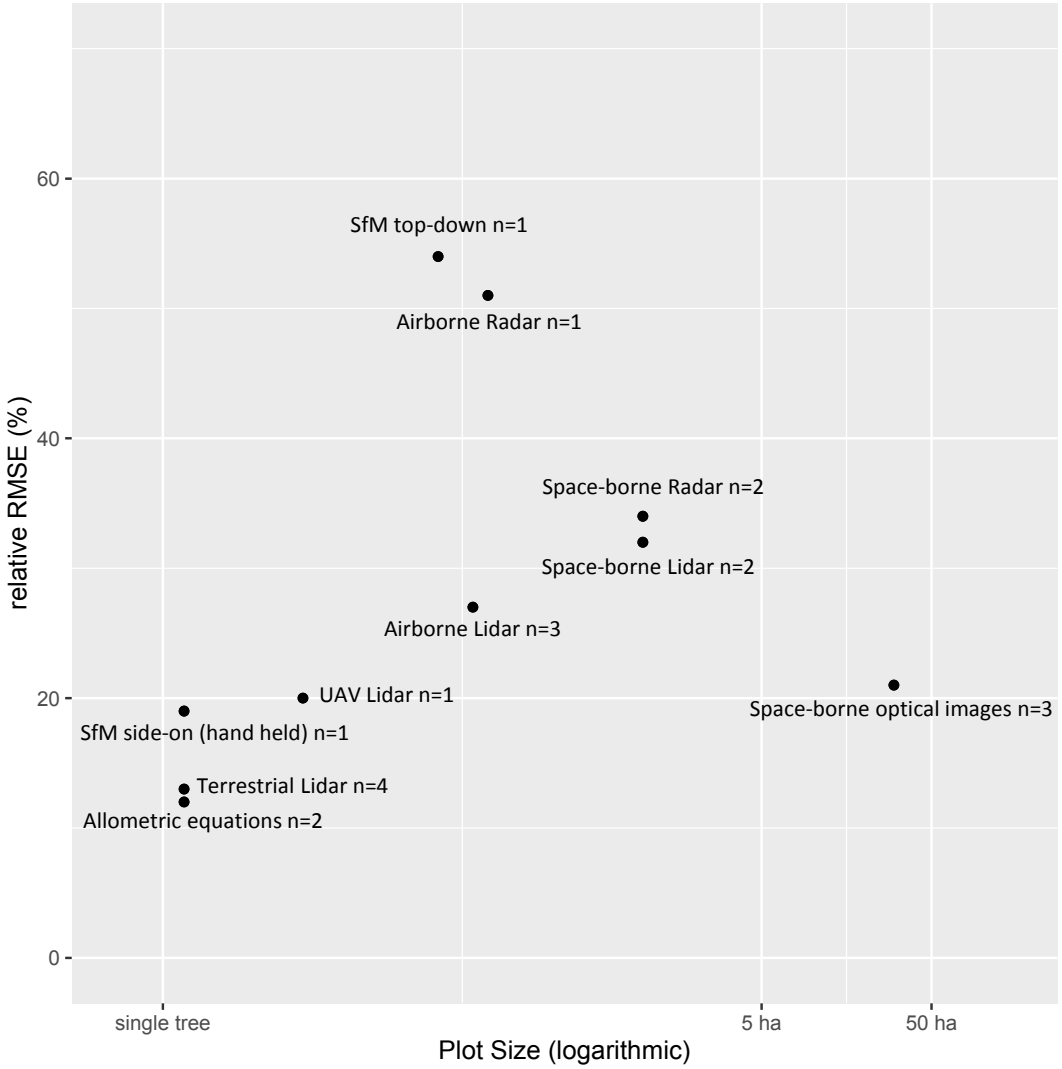

Figure 2.1: Different methods for biomass estimation of trees. Methods are positioned depending on accuracy (based on rRMSE) and on efficiency (based on observed plot sizes). Presented rRMSE values are either values from single published studies or mean values of multiple published studies. n is the number of studies. Still, rRMSE values should be compared with caution, since reference values were generated in diverse ways

Table 2.7: Classification of technical requirements and suitable forest conditions for biomass estimation techniques. See method description for details.

Technique	Grade of technical requirements	Suitable forest conditions
Allometric equations	very low	Spatial scales < 1 ha
Spaceborne Optical Images	low	Spatial scales > 10 ha, homogeneous stands, no mountain regions
Airborne Radar	very high	Spatial scales > 5 ha, homogeneous stands
Spaceborne Radar	low	Spatial scales > 10 ha, homogeneous stands
Terrestrial Lidar	high	Spatial scales < 1 ha
Airborne Lidar	very high	Spatial scales > 5 ha, most common technique
UAV Lidar	very high	Spatial scales < 5 ha
Spaceborne Lidar	low	Spatial scales > 10 ha
SfM top-down	high	Spatial scales < 5 ha
SfM side-on (hand-held)	very low	Single trees

References

D. Alves, J. V. Soares, S. Amaral, E. Mello, S. Almeida, O. F. Da Silva, and A. Silveira. Biomass of primary and secondary vegetation in Rondônia, Western Brazilian Amazon. *Global Change Biology*, 3(5):451–461, Oct. 1997. ISSN 1365-2486. doi: 10.1046/j.1365-2486.1997.00081.x.

P. Annighöfer, A. Ameztegui, C. Ammer, P. Balandier, N. Bartsch, A. Bolte, L. Coll, C. Collet, J. Ewald, N. Frischbier, T. Gebereyesus, J. Haase, T. Hamm, B. Hirschfelder, F. Huth, G. Kändler, A. Kahl, H. Kawaletz, C. Kuehne, A. Lacointe, N. Lin, M. Löf, P. Malagoli, A. Marquier, S. Müller, S. Promberger, D. Provendier, H. Röhle, J. Sathornkich, P. Schall, M. Scherer-Lorenzen, J. Schröder, C. Seele, J. Weidig, C. Wirth, H. Wolf, J. Wollmerstädt, and M. Mund. Species-specific and generic biomass equations for seedlings and saplings of European tree species. *European Journal of Forest Research*, 135(2):313–329, Jan. 2016. ISSN 1612-4669, 1612-4677. doi: 10.1007/s10342-016-0937-z. URL `http://link.springer.com/article/10.1007/s10342-016-0937-z`.

E. Baltsavias, A. Gruen, H. Eisenbeiss, L. Zhang, and L. T. Waser. High quality image matching and automated generation of 3d tree models. *International Journal of Remote Sensing*, 29(5):1243–1259, Mar. 2008. ISSN 0143-1161. doi: 10.1080/01431160701736513. URL `http://dx.doi.org/10.1080/01431160701736513`.

S. Brown, A. J. R. Gillespie, and A. E. Lugo. Biomass Estimation Methods for Tropical Forests with Applications to Forest Inventory Data. *Forest Science*, 35(4): 881–902, Dec. 1989.

K. Calders, G. Newnham, A. Burt, S. Murphy, P. Raumonen, M. Herold, D. Culvenor, V. Avitabile, M. Disney, J. Armston, and M. Kaasalainen. Nondestructive estimates of above-ground biomass using terrestrial laser scanning. *Methods in Ecology and Evolution*, 6(2):198–208, Feb. 2015. ISSN 2041-210X. doi: 10.1111/2041-210X.12301. URL `http://onlinelibrary.wiley.com/doi/10.1111/2041-210X.12301/abstract`.

J. P. Dandois and E. C. Ellis. Remote Sensing of Vegetation Structure Using Computer Vision. *Remote Sensing*, 2(4):1157–1176, Apr. 2010. doi: 10.3390/rs2041157. URL `http://www.mdpi.com/2072-4292/2/4/1157`.

M. Dassot, A. Colin, P. Santenoise, M. Fournier, and T. Constant. Terrestrial laser scanning for measuring the solid wood volume, including branches, of adult standing trees in the forest environment. *Computers and Electronics in Agriculture*, 89: 86–93, Nov. 2012. ISSN 0168-1699. doi: 10.1016/j.compag.2012.08.005. URL `http://www.sciencedirect.com/science/article/pii/S0168169912002062`.

R. O. Dubayah and J. B. Drake. Lidar Remote Sensing for Forestry. *Journal of Forestry*, 98(6):44–46, June 2000.

S. Englhart, V. Keuck, and F. Siegert. Aboveground biomass retrieval in tropical forests – The potential of combined X- and L-band SAR data use. *Remote Sensing of Environment*, 115(5):1260–1271, May 2011. ISSN 0034-4257. doi: 10.1016/j.rse.2011.01.008. URL http://www.sciencedirect.com/science/article/pii/S0034425711000216.

A. Fritz, T. Kattenborn, and B. Koch. UAV-based photogrammetric point clouds – Tree stem mapping in open stands in comparison to terrestrial laser scanner point clouds. *Int. Arch. Photogramm. Remote Sens. Spat. Inf. Sci*, 40:141–146, 2013.

A. Goetz, G. Vane, J. Solomon, and B. Rock. Imaging spectrometry for Earth remote sensing. *Science*, 228(4704):1147–1153, 1985.

P. Hyde, R. Nelson, D. Kimes, and E. Levine. Exploring LiDAR-RaDAR synergy – predicting aboveground biomass in a southwestern ponderosa pine forest using LiDAR, SAR and InSAR. *Remote Sensing of Environment*, 106(1): 28–38, Jan. 2007. ISSN 0034-4257. doi: 10.1016/j.rse.2006.07.017. URL http://www.sciencedirect.com/science/article/pii/S0034425706002781.

J. Hyyppä, O. Kelle, M. Lehikoinen, and M. Inkinen. A segmentation-based method to retrieve stem volume estimates from 3-D tree height models produced by laser scanners. *IEEE Transactions on Geoscience and Remote Sensing*, 39(5):969–975, May 2001. ISSN 0196-2892. doi: 10.1109/36.921414.

V. Kankare, M. Holopainen, M. Vastaranta, E. Puttonen, X. Yu, J. Hyyppä, M. Vaaja, H. Hyyppä, and P. Alho. Individual tree biomass estimation using terrestrial laser scanning. *ISPRS Journal of Photogrammetry and Remote Sensing*, 75: 64–75, Jan. 2013. ISSN 0924-2716. doi: 10.1016/j.isprsjprs.2012.10.003. URL http://www.sciencedirect.com/science/article/pii/S0924271612001876.

E. S. Kasischke, J. M. Melack, and M. Craig Dobson. The use of imaging radars for ecological applications – A review. *Remote Sensing of Environment*, 59(2): 141–156, Feb. 1997. ISSN 0034-4257. doi: 10.1016/S0034-4257(96)00148-4. URL http://www.sciencedirect.com/science/article/pii/S0034425796001484.

Q. M. Ketterings, R. Coe, M. van Noordwijk, Y. Ambagau', and C. A. Palm. Reducing uncertainty in the use of allometric biomass equations for predicting above-ground tree biomass in mixed secondary forests. *Forest Ecology and Management*, 146(1–3): 199–209, June 2001. ISSN 0378-1127. doi: 10.1016/S0378-1127(00)00460-6. URL http://www.sciencedirect.com/science/article/pii/S0378112700004606.

A. Komiyama, S. Poungparn, and S. Kato. Common allometric equations for estimating the tree weight of mangroves. *Journal of Tropical Ecology*, 21(04):471–477, July 2005. ISSN 0266-4674, 1469-7831. doi: 10.1017/S0266467405002476.

A. Komiyama, J. E. Ong, and S. Poungparn. Allometry, biomass, and productivity of mangrove forests: A review. *Aquatic Botany*, 89(2):128–137,

Aug. 2008. ISSN 0304-3770. doi: 10.1016/j.aquabot.2007.12.006. URL http://www.sciencedirect.com/science/article/pii/S0304377007001829.

F. Leberl, A. Irschara, T. Pock, P. Meixner, M. Gruber, S. Scholz, and A. Wiechert. Point Clouds. *Photogrammetric Engineering & Remote Sensing*, 76(10):1123–1134, Oct. 2010. doi: 10.14358/PERS.76.10.1123.

M. A. Lefsky, D. J. Harding, M. Keller, W. B. Cohen, C. C. Carabajal, F. Del Bom Espirito-Santo, M. O. Hunter, and R. de Oliveira. Estimates of forest canopy height and aboveground biomass using ICESat. *Geophysical Research Letters*, 32(22):L22S02, Nov. 2005. ISSN 1944-8007. doi: 10.1029/2005GL023971. URL http://onlinelibrary.wiley.com/doi/10.1029/2005GL023971/abstract.

K. Lim, P. Treitz, M. Wulder, B. St-Onge, and M. Flood. LiDAR remote sensing of forest structure. *Progress in Physical Geography*, 27(1):88–106, Mar. 2003. ISSN 14770296, 03091333. doi: 10.1191/0309133303pp360ra. URL http://ppg.sagepub.com/cgi/doi/10.1191/0309133303pp360ra.

Y. Lin, J. Hyyppa, and A. Jaakkola. Mini-UAV-Borne LIDAR for Fine-Scale Mapping. *IEEE Geoscience and Remote Sensing Letters*, 8(3):426–430, May 2011. ISSN 1545-598X, 1558-0571. doi: 10.1109/LGRS.2010.2079913. URL http://ieeexplore.ieee.org/lpdocs/epic03/wrapper.htm?arnumber=5624563.

T. Mette, K. Papathanassiou, and I. Hajnsek. Biomass estimation from polarimetric SAR interferometry over heterogeneous forest terrain. *Geoscience and Remote Sensing Symposium, 2004. IGARSS '04. Proceedings. 2004 IEEE International*, 1: 511–514, Sept. 2004. doi: 10.1109/IGARSS.2004.1369076.

J. Miller, J. Morgenroth, and C. Gomez. 3d modelling of individual trees using a handheld camera: Accuracy of height, diameter and volume estimates. *Urban Forestry & Urban Greening*, 14(4):932–940, 2015. ISSN 16188667. doi: 10.1016/j.ufug.2015.09.001. URL http://linkinghub.elsevier.com/retrieve/pii/S1618866715001223.

E. T. A. Mitchard, S. S. Saatchi, I. H. Woodhouse, G. Nangendo, N. S. Ribeiro, M. Williams, C. M. Ryan, S. L. Lewis, T. R. Feldpausch, and P. Meir. Using satellite radar backscatter to predict above-ground woody biomass: A consistent relationship across four different African landscapes. *Geophysical Research Letters*, 36(23):1–6, Dec. 2009. ISSN 1944-8007. doi: 10.1029/2009GL040692. URL http://onlinelibrary.wiley.com/doi/10.1029/2009GL040692/abstract.

P. Muukkonen. Generalized allometric volume and biomass equations for some tree species in Europe. *European Journal of Forest Research*, 126(2):157–166, Feb. 2007. ISSN 1612-4669, 1612-4677. doi: 10.1007/s10342-007-0168-4. URL http://link.springer.com/article/10.1007/s10342-007-0168-4.

P. Muukkonen and J. Heiskanen. Estimating biomass for boreal forests using ASTER satellite data combined with standwise forest inventory data. *Remote Sensing of Environment*, 99(4):434–447, Dec. 2005. ISSN 0034-4257. doi: 10.1016/j.rse.2005.09.011. URL http://www.sciencedirect.com/science/article/pii/S0034425705003068.

P. Muukkonen and J. Heiskanen. Biomass estimation over a large area based on standwise forest inventory data and ASTER and MODIS satellite data: A possibility to verify carbon inventories. *Remote Sensing of Environment*, 107 (4):617–624, Apr. 2007. ISSN 00344257. doi: 10.1016/j.rse.2006.10.011. URL http://linkinghub.elsevier.com/retrieve/pii/S003442570600407X.

B. W. Nelson, R. Mesquita, J. L. G. Pereira, S. Garcia Aquino de Souza, G. Teixeira Batista, and L. Bovino Couto. Allometric regressions for improved estimate of secondary forest biomass in the central Amazon. *Forest Ecology and Management*, 117(1–3):149–167, May 1999. ISSN 0378-1127. doi: 10.1016/S0378-1127(98)00475-7. URL http://www.sciencedirect.com/science/article/pii/S0378112798004757.

F. Nex and F. Remondino. UAV for 3d mapping applications: a review. *Applied Geomatics*, 6(1):1–15, Mar. 2014. ISSN 1866-9298, 1866-928X. doi: 10.1007/s12518-013-0120-x. URL http://link.springer.com/10.1007/s12518-013-0120-x.

J. P. M. Overman, H. J. L. Witte, and J. G. Saldarriaga. Evaluation of Regression Models for Above-Ground Biomass Determination in Amazon Rainforest. *Journal of Tropical Ecology*, 10(2):207–218, 1994.

N. Pfeifer, G. Mandlburger, P. Glira, A. Roncat, W. Mücke, and A. Zlinszky. Lidar: Exploiting the Versatility of a Measurement Principle in Photogrammetry. *Photogrammetric Week '15*, pages 105–118, 2015.

P. Ploton, R. Pélissier, C. Proisy, T. Flavenot, N. Barbier, S. N. Rai, and P. Couteron. Assessing aboveground tropical forest biomass using Google Earth canopy images. *Ecological Applications*, 22(3):993–1003, Apr. 2012. ISSN 1939-5582. doi: 10.1890/11-1606.1. URL http://onlinelibrary.wiley.com/doi/10.1890/11-1606.1/abstract.

S. C. Popescu. Estimating biomass of individual pine trees using airborne lidar. *Biomass and Bioenergy*, 31(9):646–655, Sept. 2007. ISSN 0961-9534. doi: 10.1016/j.biombioe.2007.06.022. URL http://www.sciencedirect.com/science/article/pii/S0961953407001316.

S. C. Popescu, K. Zhao, A. Neuenschwander, and C. Lin. Satellite lidar vs. small footprint airborne lidar: Comparing the accuracy of aboveground biomass estimates and forest structure metrics at footprint level. *Remote Sensing of Environment*, 115 (11):2786–2797, Nov. 2011. ISSN 0034-4257. doi: 10.1016/j.rse.2011.01.026. URL http://www.sciencedirect.com/science/article/pii/S0034425711001325.

K. J. Ranson, S. Saatchi, and G. Sun. Boreal forest ecosystem characterization with SIR-C/XSAR. *IEEE Transactions on Geoscience and Remote Sensing*, 33(4):867–876, July 1995. ISSN 0196-2892. doi: 10.1109/36.406673.

P. Raumonen, E. Casella, K. Calders, S. Murphy, M. Åkerbloma, and M. Kaasalainen. Massive-scale tree modelling from TLS data. *ISPRS Annals of Photogrammetry, Remote Sensing and Spatial Information Sciences*, II-3/W4:189–196, Mar. 2015. ISSN 2194-9050. doi: 10.5194/isprsannals-II-3-W4-189-2015.

S. A. Sader, R. B. Waide, W. T. Lawrence, and A. T. Joyce. Tropical forest biomass and successional age class relationships to a vegetation index derived from Landsat TM data. *Remote Sensing of Environment*, 28:143IN1159–156IN2198, 1989. URL http://www.sciencedirect.com/science/article/pii/0034425789901120.

M. D. C. Schmitt and D. F. Grigal. Generalized biomass estimation equations for *Betula papyrifera* Marsh. *Canadian Journal of Forest Research*, 11(4):837–840, Dec. 1981. ISSN 0045-5067, 1208-6037. doi: 10.1139/x81-122. URL http://www.nrcresearchpress.com/doi/abs/10.1139/x81-122.

M. Segura, M. Kanninen, and D. Suárez. Allometric models for estimating aboveground biomass of shade trees and coffee bushes grown together. *Agroforestry Systems*, 68(2):143–150, June 2006. ISSN 0167-4366, 1572-9680. doi: 10.1007/s10457-006-9005-x. URL http://link.springer.com/article/10.1007/s10457-006-9005-x.

W. Tao, Y. Lei, and P. Mooney. Dense point cloud extraction from UAV captured images in forest area. *2011 IEEE International Conference on Spatial Data Mining and Geographical Knowledge Services (ICSDM)*, pages 389–392, June 2011. doi: 10.1109/ICSDM.2011.5969071.

B. Telenius and T. Verwijst. The influence of allometric variation, vertical biomass distribution and sampling procedure on biomass estimates in commercial short-rotation forests. *Bioresource Technology*, 51(2–3):247–253, 1995. ISSN 0960-8524. doi: 10.1016/0960-8524(94)00133-L. URL http://www.sciencedirect.com/science/article/pii/096085249400133L.

A. K. Tiwari and J. S. Singh. Mapping forest biomass in India through aerial photographs and nondestructive field sampling. *Applied Geography*, 4(2):151–165, Apr. 1984. ISSN 0143-6228. doi: 10.1016/0143-6228(84)90019-5. URL http://www.sciencedirect.com/science/article/pii/0143622884900195.

T. L. Toan, S. Quegan, I. Woodward, M. Lomas, N. Delbart, and G. Picard. Relating Radar Remote Sensing of Biomass to Modelling of Forest Carbon Budgets. *Climatic Change*, 67(2-3):379–402, Dec. 2004. ISSN 0165-0009, 1573-1480. doi: 10.1007/s10584-004-3155-5. URL http://link.springer.com/article/10.1007/s10584-004-3155-5.

T. Tokola and J. Heikkilä. Improving satellite image based forest inventory by using a priori site quality information. *Silva Fennica*, 31(1):67–78, 1997. ISSN 0037-5330. URL https://helda.helsinki.fi/handle/1975/8511.

E. Tomppo, M. Nilsson, M. Rosengren, P. Aalto, and P. Kennedy. Simultaneous use of Landsat-TM and IRS-1c WiFS data in estimating large area tree stem volume and aboveground biomass. *Remote Sensing of Environment*, 82(1):156–171, Sept. 2002. ISSN 0034-4257. doi: 10.1016/S0034-4257(02)00031-7. URL http://www.sciencedirect.com/science/article/pii/S0034425702000317.

C. Uhl, R. Buschbacher, and E. A. S. Serrao. Abandoned Pastures in Eastern Amazonia. I. Patterns of Plant Succession. *The Journal of Ecology*, 76

(3):663–681, Sept. 1988. ISSN 00220477. doi: 10.2307/2260566. URL http://www.jstor.org/stable/2260566?origin=crossref.

C. Véga, U. Vepakomma, J. Morel, J.-L. Bader, G. Rajashekar, C. Jha, J. Ferêt, C. Proisy, R. Pélissier, and V. Dadhwal. Aboveground-Biomass Estimation of a Complex Tropical Forest in India Using Lidar. *Remote Sensing*, 7(8): 10607–10625, Aug. 2015. ISSN 2072-4292. doi: 10.3390/rs70810607. URL http://www.mdpi.com/2072-4292/7/8/10607/.

L. Wallace, A. Lucieer, C. Watson, and D. Turner. Development of a UAV-LiDAR System with Application to Forest Inventory. *Remote Sensing*, 4(6):1519–1543, May 2012. doi: 10.3390/rs4061519. URL http://www.mdpi.com/2072-4292/4/6/1519.

C. Wang. Biomass allometric equations for 10 co-occurring tree species in Chinese temperate forests. *Forest Ecology and Management*, 222(1-3):9–16, Feb. 2006. ISSN 03781127. doi: 10.1016/j.foreco.2005.10.074. URL http://linkinghub.elsevier.com/retrieve/pii/S0378112705005888.

T. Yao, X. Yang, F. Zhao, Z. Wang, Q. Zhang, D. Jupp, J. Lovell, D. Culvenor, G. Newnham, W. Ni-Meister, C. Schaaf, C. Woodcock, J. Wang, X. Li, and A. Strahler. Measuring forest structure and biomass in New England forest stands using Echidna ground-based lidar. *Remote Sensing of Environment*, 115 (11):2965–2974, Nov. 2011. ISSN 0034-4257. doi: 10.1016/j.rse.2010.03.019. URL http://www.sciencedirect.com/science/article/pii/S003442571100143X.

X. Yu, X. Liang, J. Hyyppä, V. Kankare, M. Vastaranta, and M. Holopainen. Stem biomass estimation based on stem reconstruction from terrestrial laser scanning point clouds. *Remote Sensing Letters*, 4(4):344–353, Apr. 2013. ISSN 2150-704X. doi: 10.1080/2150704X.2012.734931. URL http://dx.doi.org/10.1080/2150704X.2012.734931.

P. J. Zarco-Tejada, R. Diaz-Varela, V. Angileri, and P. Loudjani. Tree height quantification using very high resolution imagery acquired from an unmanned aerial vehicle (UAV) and automatic 3d photo-reconstruction methods. *European Journal of Agronomy*, 55:89–99, Apr. 2014. ISSN 1161-0301. doi: 10.1016/j.eja.2014.01.004. URL http://www.sciencedirect.com/science/article/pii/S1161030114000069.

3 Dry biomass estimation of hedge banks: Allometric equation vs. Structure from Motion via Unmanned Aerial Vehicle

Stefan Lingner, Eiko Thiessen, Kerrin Müller, Eberhard Hartung

published in *Journal of Forest Science* 64 (2018) 149–156

3.1 Abstract

The wood yield of hedge banks is very heterogeneous and hard to estimate in advance. The aim of the present study was to estimate the dry biomass of hedge banks shortly before harvesting using two different non-destructive approaches:

- allometric equation based on Diameter at Breast Height (DBH)
- volume calculations based on Structure from Motion (SfM)

and to compare these estimations with the results of the (invasive) reference method: weighing after harvesting. Study objects were three different 100 m hedge banks in Schleswig-Holstein, Germany that were divided into 10 m segments (n = 30). These segments were harvested and weighed separately to calculate dry biomass. The allometric equation yielded a relative root mean square error (rRMSE) of 32.4 %. The SfM volume models yielded an rRMSE of 30.0 %. These results indicate that SfM approaches are comparably precise to allometric equations for dry mass estimations of hedge banks. SfM approaches are less time consuming but have higher technical requirements.

3.2 Introduction

According to the European Renewable Energy Directive (2009/28/EG) renewable energy is supposed to cover at least 20 % of the gross energy consumption in 2020 within the European Union. In Germany, the amount of woody biomass used as a source for energy has already increased during the last decades (Mantau, 2012). The future demand for woody biomass could in part be supplied by existing hedge banks (Isensee et al., 2000; Seidel et al., 2015). The total length of hedge banks in Schleswig-Holstein is assumed to be around 46,000 km (Eigner, 1982).

Hedge banks as field margins are an important factor for biodiversity in agricultural landscapes (Marshall, 2002, 2004). They serve as habitat, shelter and migration path for numerous species. To preserve this ecological value the hedge banks need to be artificially maintained (Roßkamp, 2001; Ministerium für Energiewende, Landwirtschaft, Umwelt und ländliche Räume des Landes Schleswig-Holstein, 2017). This maintenance mainly consists of full cutting back in intervals of 10 to 15 years with only a few trees left standing. This cutting back allows shrubs to prevail, which in turn serve as shelter and breeding ground for numerous animals.

To date no reliable and time efficient (non-destructive) method exists to estimate the potential woody biomass of single hedge banks. Biomass estimations based on allometric equations usually are more accurate compared to remote sensing techniques, however they are very time consuming (Dittmann et al., 2017). Remote sensing techniques like Lidar or Structure from Motion (SfM) for point cloud generation could be considered on the spatial scale of single hedge banks. The present study focuses on the utilization of SfM, due to its lower technical effort. SfM is a remote sensing technique that constructs 3D point clouds from numerous overlapping photos. The underlying algorithms use methods of computer vision and photogrammetry. These algorithms are looking for key points in individual photos and are matching these points with associated key points in other photos. Thus, the camera position and its

calibration plus the location of the key points are estimated. Afterwards these key points are converted into a 3D point cloud (Snavely et al., 2007; Turner et al., 2012).

For tree parameter estimation SfM top-down approaches of leafy trees (Dandois and Ellis, 2010; Tao et al., 2011; Fritz et al., 2013; Zarco-Tejada et al., 2014; Díaz-Varela et al., 2015) and SfM side-on approaches of bald trees (Miller et al., 2015) have been applied. SfM at bald trees allows the reconstruction of pure wood and thus supposingly achieves high accuracies. However by now pure wood reconstruction has only been applied successfully to single trees Miller et al. (2015). SfM at leafy trees for height estimations or coarse volume models is less accurate but can be applied to grouped trees as well (Dandois and Ellis, 2010; Fritz et al., 2013; Zarco-Tejada et al., 2014).

In the present study dry biomasses of 30 segments in three different hedge banks were determined separately by weighing after harvesting. These reference values were compared with both biomass values estimated shortly before harvesting by an allometric equation based on DBH and with volume calculations based on SfM.

3.3 Methods

Study objects

Data for the present study were sampled in 2016 at three different hedge banks in the Schleswig-Holstein Uplands, northern Germany (54°14' N, 10°24' E). Average yearly temperature is around 10° C and annual precipitation is around 750 mm. The aim was to select three hedge banks that vary in orientation, width, species composition and dry mass yield. Figure 3.1 presents an aerial image of hedge bank 3 as an example of a typical hedge bank in the study region. A representative length of 100 m was selected for each hedge bank. Each of these 100 m objects was further divided into 10 m segments. In each of these 30 segments shrubs and trees were inventoried. SfM volume models were generated per segment.

Reference data

Shrubs and trees of the three hedge banks were felled, chopped to woodchips and weighed segment-wise with a telescopic handler. Leaves did not contribute to this total aboveground biomass due to the harvesting time in late winter. The telescopic handler had a measurement resolution of 50 kg. From each 10 m segment three samples of woodchips (approximately 5 liter each) were taken. These samples were dried at 103° C to constant weight for dry mass content estimation. Thus the dry mass of each segment could be estimated. Usually not all trees are felled in hedge banks. Some trees are left standing for ecological reasons. However these trees were already recorded by the camera and were part of the volume models. Consequently the dry masses of the trees left standing were estimated based on species-specific allometric equations provided by Zianis et al. (2005). These dry masses were added to the harvested dry masses to gain reference dry masses.

Figure 3.1: Hedge bank 3 photographed by the unmanned aerial vehicle (UAV) as an example of a typical hedge bank in the study region

Biomass estimation based on allometric equation

In each 10 m segment all shoots of shrubs and trees higher than 1 m were assessed. The assessments per shoot included:

- the determination of the species,
- the record of the DBH if the DBH was larger than 10 cm.

Usually shoots with a DBH larger than 10 cm are considered for allometric equations (Sader et al., 1989; Mitchard et al., 2009; Ploton et al., 2012). Consequently, in the present study all DBH larger than 10 cm were recorded in DBH_i, $i = 1...n_L$. DBH smaller than 10 cm were not recorded but counted in n_S. Equation 3.1 was fitted to obtain estimates for the coefficients a, b and c with a Nonlinear Least Squares Model (R function nls). The fitting was performed with the 30 reference dry masses DM and the shoot information of the corresponding segments. Equation 3.1 allows increasing weights with increasing DBH but assumes that all shrubs and trees with a DBH smaller than 10 cm have the same weight:

$$\frac{DM}{kg} = \left(\sum_{i=1}^{n} a \cdot \left(\frac{DBH_i}{cm} \right)^b \right) + c \cdot n_s \tag{3.1}$$

Table 3.1: Examples of flight heights and flight distances to hedge bank. Exact heights and distances depended on hedge bank size and ground relief

Height (m)	Distance to hedge bank (m)
10	30
17	25
24	18
30	10

Biomass estimation based on SfM volume

For image acquisition an HT-8 C180 unmanned aerial vehicle (Height-Tech, Germany) equipped with a Sony Alpha 7 camera (Sony Corporation, Japan), 24 megapixels, 30 mm lens (Zeiss, Germany) was used. This camera and lens combination resulted in a pixel size of 6 mm × 6 mm at a distance of 30 m. The octocopter was programmed and flew automatically along each hedge bank at both sides in multiple different heights (Table 3.1). Flights were performed in October and November 2016 with most of the trees still leafy. Approximately every second metre a photo was taken. This resulted in an overlap of more than 90 % between collected images. The SfM algorithm was performed in Agisoft Photoscan (Version 1.2.6, 2016). Overlapping images of the individual hedge banks were processed to point clouds (alignment: highest; dense cloud: lowest). Then these point clouds were further processed in Matlab (Version R2017a). The switch to Matlab was done, since the volume calculation in Agisoft Photoscan has limited options and cannot be run segment-wise automatically. Point cloud processing in Matlab included filtering based on k-nearest neighbours, segmenting and volume calculation (Figure 3.2). For volume calculation all points were used for polyhedron construction up to a maximum edge length of 2.5 m.

Data handling, statistics and graphics

Data handling, statistics and graphics were performed in R (R Core R Core Team, 2015) using the packages xlsx (Dragulescu, 2014), plyr (Wickham, 2011), reshape2 (Wickham, 2007), vegan (Oksanen et al., 2015), ggplot2 (Wickham, 2009) and fmsb (Nakazawa, 2017). Statistical non-intercept linear models (LM) were built for both approaches. The first model tested the effect of allometric estimated dry mass on reference dry mass. The second model tested the effect of volume on reference dry mass. In both models different coefficients per hedge bank were allowed. R^2 was calculated to compare the goodness of fit in these models. For this R^2 calculation the default equation for non-intercept models in R was used where $\hat{y}_i$ is the estimated value (Equation 3.2).

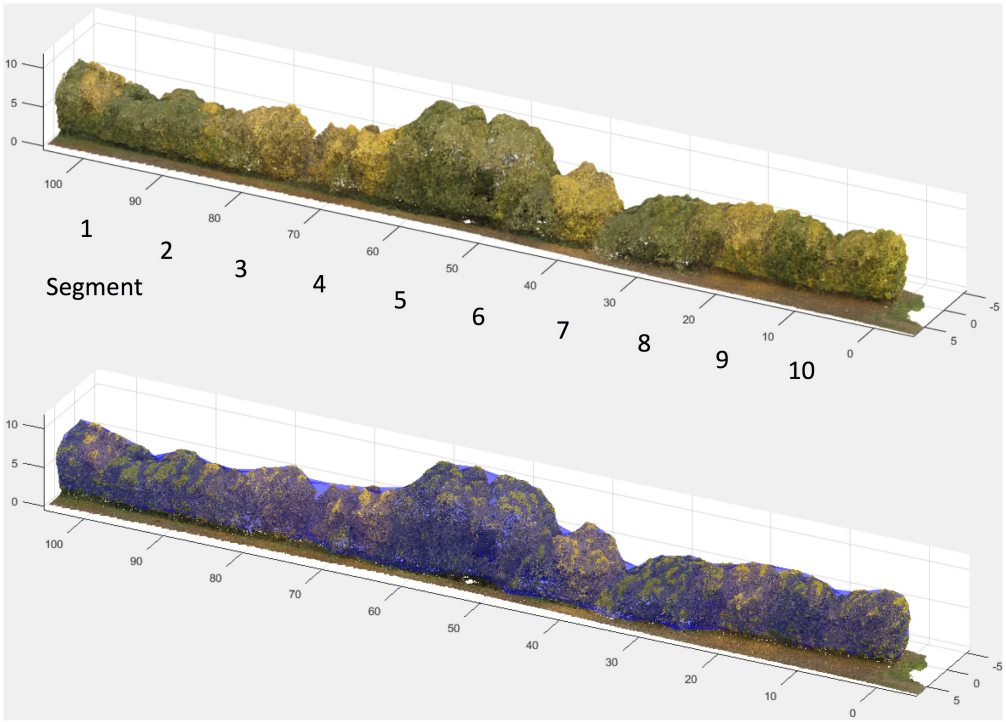

Figure 3.2: Point cloud and volume model of hedge bank 3 and its 10 segments (distances in metres)

$$R^2 = 1 - \frac{\sum_{i=1}^{n} (y_i - \hat{y}_i)^2}{\sum_{i=1}^{n} y_i^2} \tag{3.2}$$

The absolute root mean square error (RMSE) or relative root mean square error (rRMSE) is the standard accuracy estimate for the comparison of different methods of biomass estimation (Segura et al., 2006; Hyde et al., 2007; Popescu et al., 2011). Consequently this accuracy estimate was used in this study as well. The formula for the rRMSE is presented in Equation 3.3 where $\bar{y}$ is the mean value and n the sample size:

$$rRMSE = \frac{\sqrt{\frac{1}{n}\sum_{i=1}^{n} (y_i - \hat{y}_i)^2}}{\bar{y}} \tag{3.3}$$

3.4 Results

Study objects

Hedge bank 1 and 2 had an orientation from west to east while hedge bank 3 had an orientation from north to south. Typical width was 3.5 m for hedge banks 1 and 2. Hedge bank 1 was 1.5 m wide. All three hedge banks consisted of different species compositions as presented in Figure 3.3. Blackthorn (*Prunus spinosa*), field maple (*Acer campestre*) and common hazel (*Corylus avellana*) were the most abundant species. Especially segments 6 to 10 of hedge bank 2 mainly consisted of blackthorn. Hedge bank 1 had the highest abundances of hawthorn (*Crataegus sp.*), elder (*Sambucus nigra*) and common hornbeam (*Carpinus betulus*). Hedge bank 3 was dominated by field maple.

Reference data

Fresh biomass per segment varied between 150 and 2,250 kg with a mean of 1,060 kg and a standard deviation of 460 kg. Dry mass content varied between 47 and 62 %. This resulted in harvested dry masses between 91 and 1,073 kg per segment with a mean of 583 kg and a standard deviation of 236 kg (Figure 3.4). In total six trees with a DBH larger than 10 cm were left standing as presented in Table 3.2. Their dry masses were estimated using the equations listed in Table 3.2 and added to the harvested dry masses to gain reference dry masses. These reference dry masses varied between 280 and 1,660 kg with a mean of 758 kg and a standard deviation of 334 kg.

Biomass estimation based on allometric equation

Estimated coefficients of Equation 3.1 were $a = 0.01$, $b = 2.98$ and $c = 2.40$. Figure 3.5 shows the estimated and reference dry masses per segment. In the statistical non-intercept model the coefficient for estimated dry mass was 1.00 and had a significant

Table 3.2: Trees left standing. Dry masses were estimated based on species-specific allometric equations from Zianis et al. (2005)

Hedge bank	Segment	Species	DBH (cm)	Equation	Dry biomass (kg)
1	2	*Fraxinus excelsior*	52	$DM = 0.085 \cdot DBH^{2.4882}$	1,590
1	5	*F. excelsior*	38	$DM = 0.085 \cdot DBH^{2.4882}$	729
1	8	*Quercus robur*	51	$DM = 0.089 \cdot DBH^{2.4682}$	1,453
1	10	*Q. robur*	40	$DM = 0.089 \cdot DBH^{2.4682}$	798
2	4	*Q. robur*	37	$DM = 0.089 \cdot DBH^{2.4682}$	658
3	9	*Acer campestre*	11	$DM = 0.067 \cdot DBH^{2.5751}$	32

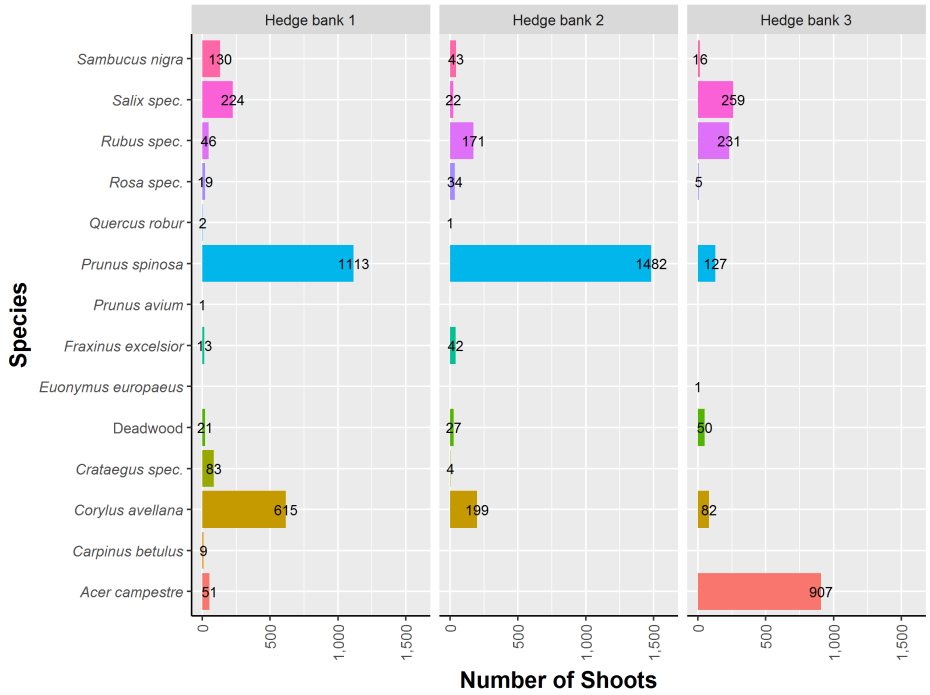

Figure 3.3: Species composition of the three hedge banks

effect (LM, $F_{1,29} = 298.1$, $p < 0.001$). The different hedge banks had no significant effect. The model achieved an R^2 of 0.91 and an rRMSE of 32.4 %. Measured DBH and counted shoots per segment are presented in Figure 3.6 and 3.7. About 98 % of all shoots had a DBH smaller than 10 cm. Transferred into weight this equals 37 % of total dry biomass if the fitting result of Equation 3.1 is applied with 2.40 kg per shoot.

Biomass estimation based on SfM volume

Calculated volumes based on SfM per segment varied between 95.5 and 957.2 m^3. Volumes versus reference dry masses are presented in Figure 3.8. In the statistical non-intercept model the interaction of volume and hedge banks was significant (LM, $F_{3,27} = 10.8$, $p < 0.001$). The equation for the statistical model is presented in Equation 3.4 with the estimated coefficients d of hedge bank i and volume V. The coefficients d for hedge bank 1, 2 and 3 were 1.94, 2.43 and 1.42 $kg \cdot m^{-3}$, respectively. This model achieved an R^2 of 0.95 and an rRMSE of 22.5 %. A simpler model with a general coefficient for volume achieved an R^2 of 0.92 and an rRMSE of 30.0 %. This general coefficient d over all hedge banks was 1.79 $kg \cdot m^{-3}$ (LM, $F_{1,29} = 18.8$, $p < 0.001$).

$$DM = d_i \cdot V \tag{3.4}$$

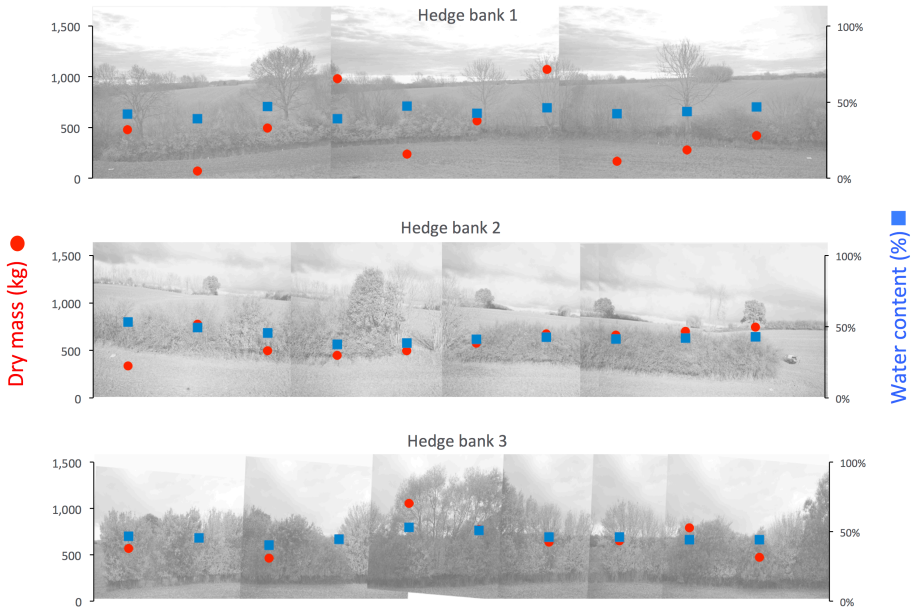

Figure 3.4: Harvested dry masses (without trees left standing) and water content (water content = 1 – dry mass content) of the three hedge banks

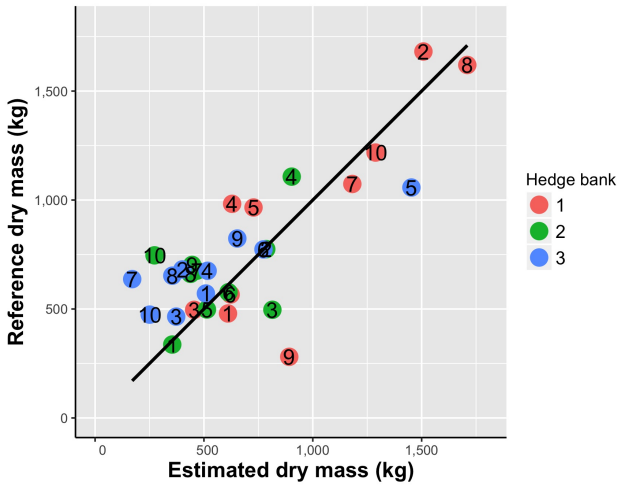

Figure 3.5: Dry masses estimated by an allometric equation based on DBH vs. reference dry masses determined by weighing of 30 segments in three hedge banks. Estimated dry masses were predicted based on Equation 3.1 with fitted parameters given in the text. The black line is a linear regression line

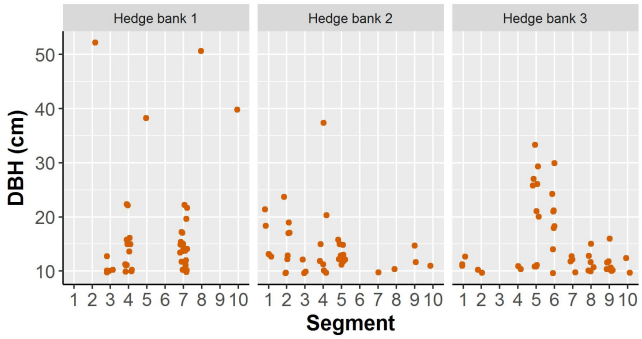

Figure 3.6: Measured DBH of trees > 10 cm in the three hedge banks

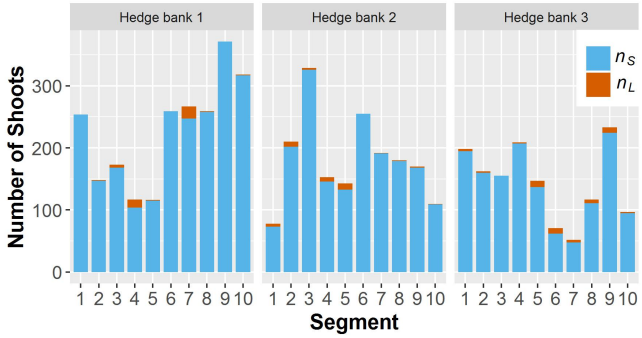

Figure 3.7: Number of shoots in the three hedge banks. n_S = number of shoots with a DBH < 10 cm, n_L = number of shoots with DBH > 10 cm

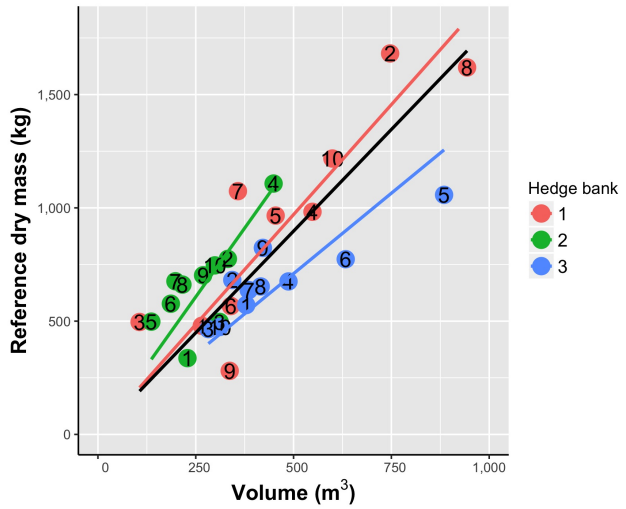

Figure 3.8: Structure from Motion based volume vs. reference dry mass of 30 segments in three hedge banks. Colored lines represent linear regression lines per hedge bank with fitted parameters given in the text. The black line represents a general regression line

3.5 Discussion and Conclusion

The selected hedge banks in the present study differed in orientation, species composition, width and wood yield. These differences indicate that the selection of heterogeneous hedge banks was successful. The samples appear to be representative of hedge banks in the Schleswig-Holstein Uplands, northern Germany.

Estimated dry mass based on allometric equations had a significant effect on reference dry mass in the statistical model. The estimated coefficient was 1. This value does not surprise since it was modeled to be 1. Different coefficients per hedge bank did not significantly improve the model. The model resulted in an rRMSE of 32.4 %. This is a lot less precise than allometric equations in literature like 9 % in Segura et al. (2006) (shade trees of coffee plants) and 13 % in Annighöfer et al. (2016) (seedlings and saplings of European tree species). Plus in the present study the same data were used for model generation and valuation. It is likely that the model fit would decrease if independent data for model generation and valuation were used. One possible reason for the relative low precision of the allometric equation approach in the present study is surely the diverse growth habit of trees in hedge banks. However the major reason is probably the weight of shrubs and trees with a DBH smaller than 10 cm. All three hedge banks had a large proportion of shoots with a DBH smaller than 10 cm. In Equation 3.1 all shrubs and trees with a DBH smaller than 10 cm were assumed to have the same weight. This assumption surely does not apply. One example is the 9^{th} segment of the 1^{st} hedge bank. The reason for its poor fit is its low weight but the large number of shoots with a DBH smaller than 10 cm. No shoot with a DBH larger than 10 cm was present in this segment. To create more realistic models it would be necessary to assess the DBH of shrubs and trees with a DBH smaller than 10 cm as well. However this would result in an enormous effort for data collection.

Volume had a significantly different effect on reference dry mass depending on the hedge bank. This pattern indicates that the relationship between volume and mass additionally depends on other factors like species composition. However due to the sample size these effects could not be tested sufficiently in the present study. The statistical model assuming a general coefficient for volume resulted in an rRMSE of 30.0 %. This rRMSE is larger than the rRMSE from Miller et al. (2015), who used SfM to calculate the volume of 30 single bald trees and received an rRMSE of 19 %. In Miller's study the single trees were photographed side-on all around. Dandois and Ellis (2010) used SfM for biomass estimation at a larger spatial scale and received an rRMSE of 54 %. However, due to the large spatial scale they used top-down photos only.

In the present study the rRMSE of the SfM approach was slightly lower than the rRMSE of the allometric approach. The R^2 was better in the volume models as well. The results of the comparison indicate that SfM approaches are generally suitable for dry mass estimations of hedge banks. SfM approaches appear to be reasonably precise and are a lot less time consuming than approaches based on allometric equations. However, technical requirements are higher when applying SfM.

References

P. Annighöfer, A. Ameztegui, C. Ammer, P. Balandier, N. Bartsch, A. Bolte, L. Coll, C. Collet, J. Ewald, N. Frischbier, T. Gebereyesus, J. Haase, T. Hamm, B. Hirschfelder, F. Huth, G. Kändler, A. Kahl, H. Kawaletz, C. Kuehne, A. Lacointe, N. Lin, M. Löf, P. Malagoli, A. Marquier, S. Müller, S. Promberger, D. Provendier, H. Röhle, J. Sathornkich, P. Schall, M. Scherer-Lorenzen, J. Schröder, C. Seele, J. Weidig, C. Wirth, H. Wolf, J. Wollmerstädt, and M. Mund. Species-specific and generic biomass equations for seedlings and saplings of European tree species. *European Journal of Forest Research*, 135(2):313–329, Jan. 2016. ISSN 1612-4669, 1612-4677. doi: 10.1007/s10342-016-0937-z. URL `http://link.springer.com/article/10.1007/s10342-016-0937-z`.

J. P. Dandois and E. C. Ellis. Remote Sensing of Vegetation Structure Using Computer Vision. *Remote Sensing*, 2(4):1157–1176, Apr. 2010. doi: 10.3390/rs2041157. URL `http://www.mdpi.com/2072-4292/2/4/1157`.

R. Díaz-Varela, R. de la Rosa, L. León, and P. Zarco-Tejada. High-Resolution Airborne UAV Imagery to Assess Olive Tree Crown Parameters Using 3d Photo Reconstruction: Application in Breeding Trials. *Remote Sensing*, 7 (4):4213–4232, Apr. 2015. ISSN 2072-4292. doi: 10.3390/rs70404213. URL `http://www.mdpi.com/2072-4292/7/4/4213/`.

S. Dittmann, E. Thiessen, and E. Hartung. Applicability of different non-invasive methods for tree mass estimation: A review. *Forest Ecology and Management*, 398: 208–215, 2017.

A. A. Dragulescu. xlsx: Read, write, format Excel 2007 and Excel 97/2000/XP/2003 files, 2014. URL `http://CRAN.R-project.org/package=xlsx`.

J. Eigner. Bewertung von Knicks in Schleswig-Holstein. *Laufener Seminarbeiträge*, 5 (82):110–117, 1982.

A. Fritz, T. Kattenborn, and B. Koch. UAV-based photogrammetric point clouds – Tree stem mapping in open stands in comparison to terrestrial laser scanner point clouds. *Int. Arch. Photogramm. Remote Sens. Spat. Inf. Sci*, 40:141–146, 2013.

P. Hyde, R. Nelson, D. Kimes, and E. Levine. Exploring LiDAR-RaDAR synergy – predicting aboveground biomass in a southwestern ponderosa pine forest using LiDAR, SAR and InSAR. *Remote Sensing of Environment*, 106(1): 28–38, Jan. 2007. ISSN 0034-4257. doi: 10.1016/j.rse.2006.07.017. URL `http://www.sciencedirect.com/science/article/pii/S0034425706002781`.

E. Isensee, D. K. Stübig, and C. Lubkowitz. Bergung und Aufbereitung von Knick- und Schwachholz. *Landtechnik–Agricultural Engineering*, 55(5):346–347, 2000.

U. Mantau. *Holzrohstoffbilanz Deutschland, Entwicklungen und Szenarien des Holzaufkommens und der Holzverwendung 1987 bis 2015*. PhD thesis, Universität Hamburg, Hamburg, 2012.

E. Marshall. Introducing field margin ecology in Europe. *Agriculture, Ecosystems & Environment*, 89(1-2):1–4, Apr. 2002. ISSN 01678809. doi: 10.1016/S0167-8809(01)00314-0.

E. J. P. Marshall. Agricultural landscapes: field margin habitats and their interaction with crop production. *Journal of Crop Improvement*, 12(1-2):365–404, 2004.

J. Miller, J. Morgenroth, and C. Gomez. 3d modelling of individual trees using a handheld camera: Accuracy of height, diameter and volume estimates. *Urban Forestry & Urban Greening*, 14(4):932–940, 2015. ISSN 16188667. doi: 10.1016/j.ufug.2015.09.001. URL http://linkinghub.elsevier.com/retrieve/pii/S1618866715001223.

Ministerium für Energiewende, Landwirtschaft, Umwelt und ländliche Räume des Landes Schleswig-Holstein. Durchführungsbestimmungen zum Knickschutz, Jan. 2017.

E. T. A. Mitchard, S. S. Saatchi, I. H. Woodhouse, G. Nangendo, N. S. Ribeiro, M. Williams, C. M. Ryan, S. L. Lewis, T. R. Feldpausch, and P. Meir. Using satellite radar backscatter to predict above-ground woody biomass: A consistent relationship across four different African landscapes. *Geophysical Research Letters*, 36(23):1–6, Dec. 2009. ISSN 1944-8007. doi: 10.1029/2009GL040692. URL http://onlinelibrary.wiley.com/doi/10.1029/2009GL040692/abstract.

M. Nakazawa. fmsb: Functions for Medical Statistics Book with some Demographic Data, 2017. URL http://CRAN.R-project.org/package=fmsb.

J. Oksanen, F. G. Blanchet, R. Kindt, P. Legendre, P. R. Minchin, R. B. O'Hara, G. L. Simpson, P. Solymos, M. H. H. Stevens, and H. Wagner. vegan: Community Ecology Package, 2015.

P. Ploton, R. Pélissier, C. Proisy, T. Flavenot, N. Barbier, S. N. Rai, and P. Couteron. Assessing aboveground tropical forest biomass using Google Earth canopy images. *Ecological Applications*, 22(3):993–1003, Apr. 2012. ISSN 1939-5582. doi: 10.1890/11-1606.1. URL http://onlinelibrary.wiley.com/doi/10.1890/11-1606.1/abstract.

S. C. Popescu, K. Zhao, A. Neuenschwander, and C. Lin. Satellite lidar vs. small footprint airborne lidar: Comparing the accuracy of aboveground biomass estimates and forest structure metrics at footprint level. *Remote Sensing of Environment*, 115 (11):2786–2797, Nov. 2011. ISSN 0034-4257. doi: 10.1016/j.rse.2011.01.026. URL http://www.sciencedirect.com/science/article/pii/S0034425711001325.

R Core Team. R: A Language and Environment for Statistical Computing, 2015. URL http://www.R-project.org/.

T. Roßkamp. Zur Bestandssituation der Hecken in Niedersachsen und deren Auswirkung auf die Vogelwelt, dargestellt an traditionellen Wallheckenlandschaften im nordwestlichen Niedersachsen. *Seevögel - Zeitschrift Verein Jordsand,*, 22(2), 2001.

S. A. Sader, R. B. Waide, W. T. Lawrence, and A. T. Joyce. Tropical forest biomass and successional age class relationships to a vegetation index derived from Landsat TM data. *Remote Sensing of Environment*, 28:143IN1159–156IN2198, 1989. URL `http://www.sciencedirect.com/science/article/pii/0034425789901120`.

M. Segura, M. Kanninen, and D. Suárez. Allometric models for estimating aboveground biomass of shade trees and coffee bushes grown together. *Agroforestry Systems*, 68(2):143–150, June 2006. ISSN 0167-4366, 1572-9680. doi: 10.1007/s10457-006-9005-x. URL `http://link.springer.com/article/10.1007/s10457-006-9005-x`.

D. Seidel, G. Busch, B. Krause, C. Bade, C. Fessel, and C. Kleinn. Quantification of Biomass Production Potentials from Trees Outside Forests – A Case Study from Central Germany. *BioEnergy Research*, 8(3):1344–1351, Sept. 2015. ISSN 1939-1234, 1939-1242. doi: 10.1007/s12155-015-9596-z. URL `http://link.springer.com/10.1007/s12155-015-9596-z`.

N. Snavely, S. M. Seitz, and R. Szeliski. Modeling the World from Internet Photo Collections. *International Journal of Computer Vision*, 80(2):189–210, Dec. 2007. ISSN 0920-5691, 1573-1405. doi: 10.1007/s11263-007-0107-3.

W. Tao, Y. Lei, and P. Mooney. Dense point cloud extraction from UAV captured images in forest area. *2011 IEEE International Conference on Spatial Data Mining and Geographical Knowledge Services (ICSDM)*, pages 389–392, June 2011. doi: 10.1109/ICSDM.2011.5969071.

D. Turner, A. Lucieer, and C. Watson. An Automated Technique for Generating Georectified Mosaics from Ultra-High Resolution Unmanned Aerial Vehicle (UAV) Imagery, Based on Structure from Motion (SfM) Point Clouds. *Remote Sensing*, 4(12):1392–1410, May 2012. ISSN 2072-4292. doi: 10.3390/rs4051392. URL `http://www.mdpi.com/2072-4292/4/5/1392/`.

H. Wickham. Reshaping Data with the reshape Package. *Journal of Statistical Software*, 21(12):1–20, 2007. URL `http://www.jstatsoft.org/v21/i12/`.

H. Wickham. *ggplot2: Elegant Graphics for Data Analysis*. Springer, New York, NY, 2009. ISBN 978-0-387-98140-6. URL `http://ggplot2.org`.

H. Wickham. The Split-Apply-Combine Strategy for Data Analysis. *Journal of Statistical Software*, 40(1):1–29, 2011. URL `http://www.jstatsoft.org/v40/i01/`.

P. J. Zarco-Tejada, R. Diaz-Varela, V. Angileri, and P. Loudjani. Tree height quantification using very high resolution imagery acquired from an unmanned aerial vehicle (UAV) and automatic 3d photo-reconstruction methods. *European Journal of Agronomy*, 55:89–99,

Apr. 2014. ISSN 1161-0301. doi: 10.1016/j.eja.2014.01.004. URL http://www.sciencedirect.com/science/article/pii/S1161030114000069.

D. Zianis, P. Muukkonen, R. Mäkipää, and M. Mencuccini. *Biomass and stem volume equations for tree species in Europe*. Number 4, 2005 in Silva Fennica monographs. Finnish Society of Forest Science, Finnish Forest Research Institute, Helsinki, Finland, 2005. ISBN 978-951-40-1983-8 978-951-40-1984-5. OCLC: ocm63646996.

4 Biomass estimation in linear forest objects: Structure from Motion vs. aerial images

Stefan Lingner, Eiko Thiessen, Eberhard Hartung

submitted to *Journal of Forest Science*

4.1 Abstract

Wood-chips of linear forest objects (hedge banks and roadside plantings) are used as sustainable energy supply in wood-chip heating systems. However, wood yield of linear forest objects is very heterogeneous and hard to estimate in advance. The aim of the present study was to compare the dry mass estimation potentials using two different non-destructive data:

- Canopy area (derived from aerial images) and mean age at stump level
- Volume of vegetation cover based on SfM (structure from motion) via UAV (unmanned aerial vehicle)

These two types of data were separately used to predict reference dry mass (ground truth) in eleven objects (5 hedge banks and 6 roadside plantings) in Schleswig-Holstein, Germany. The predicting potentials were compared afterwards. The reference dry mass was ascertained by weighing after harvesting and drying samples to constant weight.

The model predicting reference dry mass using canopy area and mean age at stump level achieved a relative RMSE of 52 % (42 % at larger plot sizes). The model predicting reference dry mass using SfM volume achieved a relative RMSE of 30 % (16 % at larger plot sizes). This result indicates that biomass is better described by volume of vegetation cover than by canopy area and age.

4.2 Introduction

According to the European Renewable Energy Directive (2009/28/EG) renewable energy is supposed to cover at least 20 % of the gross energy consumption in 2020 within the European Union. In Germany, the amount of woody biomass used as a source for energy has already increased during the last decades (Mantau, 2012). The future demand for woody biomass could in part be supplied by existing hedge banks and roadside plantings (Isensee et al., 2000; Seidel et al., 2015).

The demand of wood-chips implies the need for woody biomass predicting models. Biomass predicting models could help with logistical planning and economical estimations. Biomass predictions based on allometric equations were already compared to biomass predictions based on SfM (structure from motion) in a previous study (Lingner et al., 2018). Dry mass predictions based on SfM turned out to be comparably accurate. However SfM is time consuming and technically demanding.

SfM is a remote sensing technique that constructs 3D point clouds from numerous overlapping photos. The underlying algorithms use methods of computer vision and photogrammetry. These algorithms are looking for key points in individual photos and are matching these points with associated key points in other photos. Thus, the camera position and its calibration plus the location of the key points are estimated. Afterwards these key points are converted into a 3D point cloud (Snavely et al., 2007; Turner et al., 2012).

Predicting models based on aerial images instead of volume models would be faster processable and consequently more economical. Seidel et al. (2015) has used canopy area and age to predict dry mass in linear forest objects in Germany. In this study

the canopy areas were derived from aerial images. The growth rate was assumed to be $0.7\,kg{\cdot}m^{-2}{\cdot}a^{-1}$ where a is year.

The aim of the present study was to compare the predicting potential of these two different non-destructive approaches. The first approach used canopy area and mean age at stump level as predicting variable and the second approach used volume of vegetation cover based on SfM as predicting variable. The data of both approaches were used separately to predict reference dry mass (ground truth). Afterwards the predicting potential of both approaches was compared. In each approach two different equations were tested. The first approach was tested with the coefficient $0.7\,kg{\cdot}m^{-2}{\cdot}a^{-1}$ and with an estimated one. The second approach was tested with an equation that simply adds the volume per segment and with an equation that accounts for the height oft the vegetation additionally.

Reference dry masses was ascertained by weighing after harvesting and drying samples to constant weight. Sample plots were 110 Segments (10 m) in 11 linear forest objects in Schleswig-Holstein, Germany. These 11 linear forest objects were five hedge banks and six roadside plantings.

4.3 Methods

Study objects

Data for the present study were sampled in 2016, 2017 and 2018 at eleven linear forest objects in Schleswig-Holstein, Germany. These objects consisted of five different hedge banks (objects 1 to 5) and six roadside plantings (objects 6 to 11). A representative length of 100 m was selected for each object. All objects were divided into 10 segments of 10 m each. A Real Time Kinematic GPS (Trimble Ag 442, 2 cm horizontal accuracy) recorded the GPS coordinates of the segments' corners.

Sampled hedge banks and roadside plantings had diverse species compositions. Some of the hedge banks had a large proportion of blackthorn (*Prunus spinosa*) other objects were dominated by willow (genus *Salix*), sycamore (*Acer pseudoplatanus*) or common hornbeam (*Carpinus betulus*). Most frequent counted shoots of all segments were blackthorn, fly honeysuckle (*Lonicera xylosteum*) and common hazel (*Corylus avellana*).

Reference data

In the beginning of 2017 (Objects 1,2,6,7,8) and 2018 (Objects 3,4,5,9,10,11) shrubs and trees of each segment were felled, chopped to wood-chips and weighed segment-wise. The vegetation was without leafs at that time. Due to local conditions the segments had to be weighted on four different scales (Table 4.1).

From each segment three samples of wood-chips (approx. 5 litres each) were taken. These samples were dried at 103° C to constant weight according to DIN 52183 for dry mass content estimation. Thus the dry mass of every segment could be estimated. Usually not all trees are felled in hedge banks and roadside plantings. Some trees are left standing for ecological reasons. However these trees were part of the SfM volume models and aerial images. Consequently the dry masses of the trees left standing were estimated with species-specific allometric equations based on DBH (diameter at

breast height) provided by Zianis et al. (2005). These dry masses were added to the harvested dry masses to gain the total reference dry masses per segment.

Table 4.1: Different scales used for weighing

Year	Hedge banks (Resolution)	Roadside plantings (Resolution)
2017	Telescopic handler (50 kg)	Permanent truck scales (20 kg)
2018	Mobile truck scales (10 kg)	Permanent truck scales (20 kg)

Biomass estimation based on canopy area and age

The following prediction model is based on the idea that age could potentially be a substitute for tree height and that the canopy area could potentially be a substitute for basal area. Basal area in forest ecology is the sum of the area of all stems at breast height. Canopy area in the current paper is the area covered by the combined canopy of the segment. Consequently Equation 4.2 approximates Equation 4.1.

$$\frac{dry\,mass}{kg} = a \cdot \frac{tree\,height}{m} \cdot \frac{basal\,area}{m^2} \tag{4.1}$$

$$\frac{dry\,mass}{kg} = b \cdot \frac{age}{year} \cdot \frac{canopy\,area}{m^2} \tag{4.2}$$

The canopy areas of the segments were estimated using aerial images recorded in 2016 provided from the state government of Schleswig-Holstein. These images had a pixel resolution of 20 cm × 20 cm on ground. The canopy outlines of all 110 segments were manually digitized and canopy areas were calculated (Figure 4.1). This process was performed in QGIS. The ages of the objects were estimated after harvesting by annual ring counting of 20 representative stumps per object. The mean age per object was used as object age. This mean represents the period since the last harvest and therefore the time duration for biomass growth used in Equation 4.2. Seidel et al. (2015) recommended to estimate *dry mass* of linear forest objects based on *canopy area* and *age* using Equation 4.2 with 0.7 as prefactor b.

Two models were generated. In Model 1.1 0.7 was used as b in Equation 4.2. For Model 1.2 prefactor b was estimated anew using the 110 data points of the present study.

Biomass estimation based on SfM Volume of vegetation cover

For image acquisition an UAV (unmanned aerial vehicle) (HT-8 C180) equipped with a camera (Sony Alpha 7, 24 megapixels, 30 mm Zeiss lens) was used. This camera and lens combination resulted in a pixel size of 6 mm × 6 mm at a distance of 30 m. The octocopter was programmed and flew automatically above and along each object in multiple different heights (described in Lingner et al. (2018)). At the hedge banks the octocopter could fly above the object and on both sides. However at the roadside plantings the octocopter could only fly on the opposite side of the road and above the object due to safety reasons.

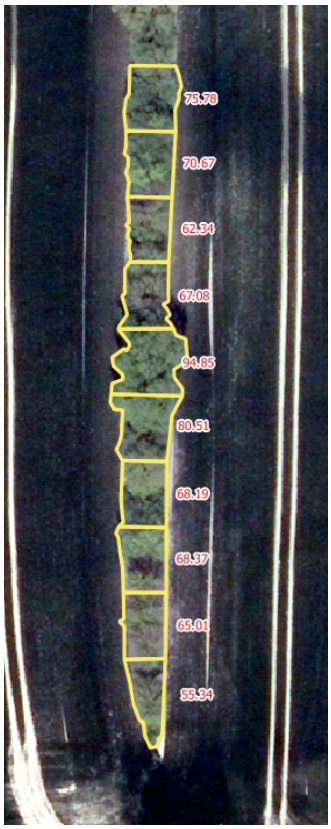

Figure 4.1: Manually digitized hedge bank and canopy area calculation

The UAV flights were performed in the second half of 2016 (Objects 1,2,6,7,8) and in the second half of 2017 (Objects 3,4,5,9,10,11) with most of the trees still leafy. Approximately every two metres a photo was taken. This resulted in an overlap of more than 90 % between collected images. Images were processed in AgisoftPhotoscan (Version 1.2.6) for point cloud generation (Alignment: highest; Dense cloud: lowest) (Figure 4.2a). Then these point clouds were processed in Matlab (Version R2017a). The point cloud processing in Matlab included ground level estimation and volume calculation. For volume calculation square tiles with a uniform tile edge length (see below) were fitted at the estimated ground level. These tiles were used as base for pillars that reached from the estimated ground level to the highest point above the specific tile (Figure 4.2b).

Square tiles with different edge lengths were tested on a sub sample to find the best suitable tile edge length. Tested tile edge lengths were d/n ($n = 1 \ldots 15$) to fit exactly into the segments with a length of $d = 10\,\mathrm{m}$.

Two different models were generated for biomass estimation based on Volume. In Model 2.1 the volumes of the pillars V_i were simply added segment wise yielding to the total volume $SV_j = \sum V_i$ of segment j. These segment volumes SV_j were modelled against reference $dry\,mass_j$ in Equation 4.3. Model 2.1 was generated for every tested tile edge length to find the best fitting tile edge length based on rRMSE. This best fitting tile edge length was used for further analysis (Model 2.1 and 2.2).

$$\frac{dry\,mass_j}{kg} = c \cdot \frac{SV_j}{m^3} \tag{4.3}$$

For Model 2.2 Equation 4.4 was fitted to obtain estimates for factor d and exponent f, where V_i is pillar volume and j is the segment number. This equation allows for different volume specific densities depending on pillar height. This could possibly rather represent the natural growth habit of trees then Equation 4.3. Due to the fact that higher trees usually have a thicker stem than smaller trees, a higher pillar probably has a higher wood-air-ratio than a smaller pillar.

$$\frac{dry\,mass_j}{kg} = d \cdot \sum_{i=1}^{Number\,V\,in\,j} \left(\frac{V_i}{m^3}\right)^f \tag{4.4}$$

Different plot sizes

When the trees were weighed segment-wise it was often hard to decide to which segment a tree belonged. Especially at the borders of the segments it was challenging to assign all trees to a distinct segment. Plus, if the crown of a tree covered parts of two adjacent segments the tree was not split apart. These border errors resulted by assigning trees to the wrong segment probably results in wrong reference data. It was tried to decrease these border errors test-wise by using larger plot sizes for both Model 1.2 (canopy area & age) and Model 2.1 (volume). Compared additional plot lengths were 20 m, 50 m, and 100 m.

To evaluate the accuracy of both biomass estimation approaches for applications in the field the 95 % confidence intervals of the standard deviation (CI_{SD}) were calculated. These two CI_{SD} were calculated using the residuals of Model 1.2 and 2.1. Afterwards each CI_{SD} was converted into a relative CI_{SD} by dividing it by the mean

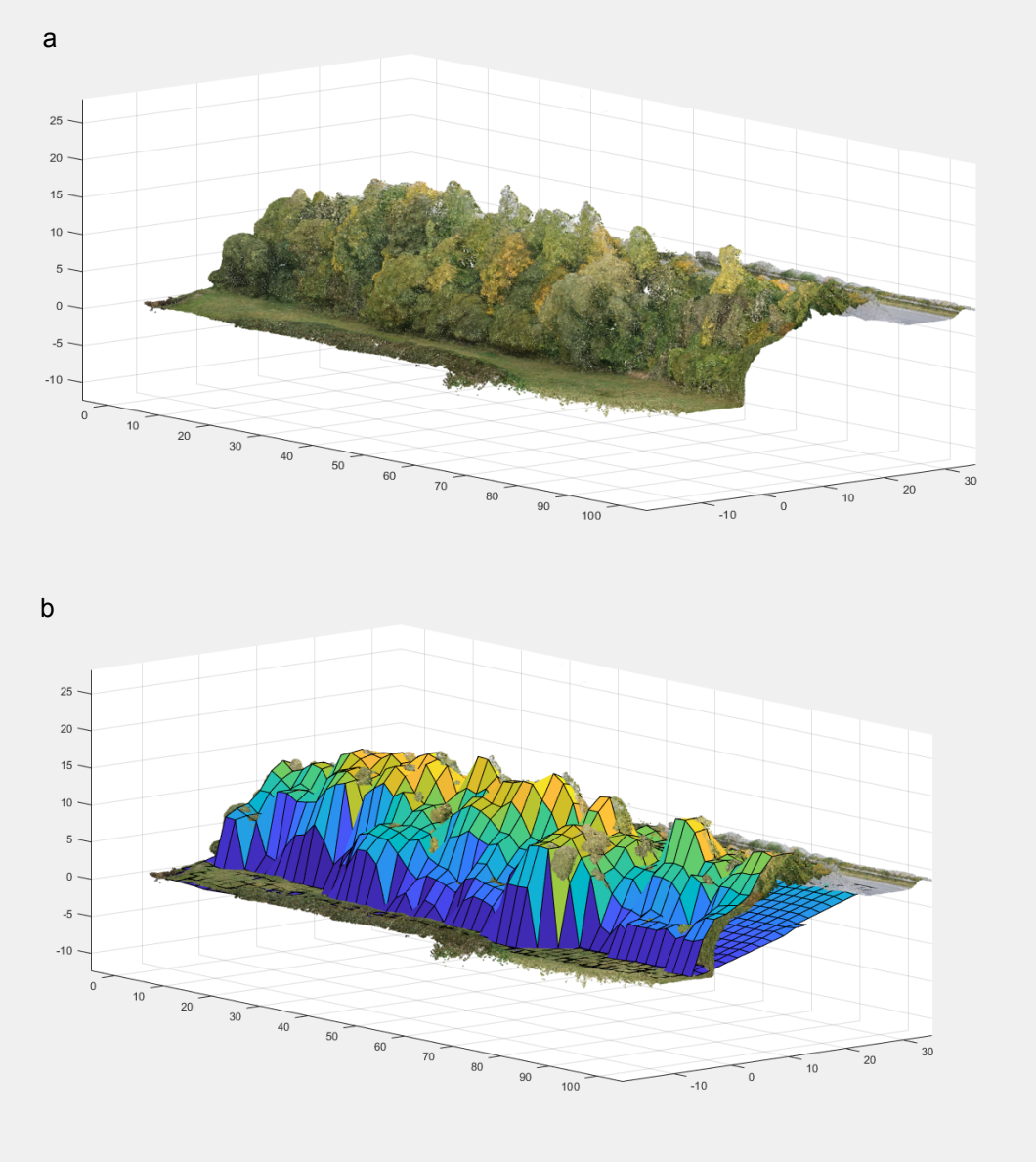

Figure 4.2: a) Point cloud of roadside planting. b) Point cloud with estimated ground level and pillars for volume calculation

reference dry biomass. For this calculation the plots with a length of 100 m were used since these plot sizes are common at applications in the field.

Data handling, statistics and graphics

The RMSE (absolute root mean square error) or rRMSE (relative root mean square error) is the standard accuracy estimate for the comparison of different methods of biomass estimation (Hyde et al., 2007; Popescu et al., 2011; Segura et al., 2006). Consequently this accuracy estimate was used in this study as well. The formula for the rRMSE is presented in Equation 4.5 where $\bar{y}$ is the mean value and $\hat{y}$ the expected value.

$$rRMSE = \frac{\sqrt{\frac{1}{n}\sum_{i=1}^{n}(y_i - \hat{y_i})^2}}{\bar{y}} \tag{4.5}$$

Data handling, statistics and graphics were performed in R (R Core Team, 2015) using the packages xlsx (Dragulescu, 2014), plyr (Wickham, 2011), mgcv (Wood, 2011) and ggplot2 (Wickham, 2009).

4.4 Results

Reference data

Fresh biomass per segment varied between 380 and 8380 kg (Figure 4.3) and dry biomass content varied between 47 % and 66 %. This resulted in harvested dry biomasses between 237 and 4649 kg (Figure 4.4). In total 66 trees with a DBH larger than 10 cm were left standing. Their dry masses were estimated with equations from Zianis et al. (2005) (Figure 4.5) and added to the harvested dry biomasses to gain reference dry biomasses (Figure 4.6). These reference dry biomasses varied between 243 und 4800 kg. The mean estimated dry mass of the trees left standing per segment was around 9 % of the reference dry mass.

Biomass estimation based on canopy area and age

Digitizes canopy areas per segment varied between 30 and 258 m^2. The mean age of the objects ranged from 13 to 32 years. Ages and canopy areas are displayed in (Figure 4.7). Estimated prefactor b in Model 1.2 was 0.44.

Figure 4.8 shows both the estimated dry biomass with a prefactor b of 0.7 (Model 1.1) and the estimated dry biomass with the calculated prefactor b of 0.44 (Model 1.2). Model 1.1 resulted in an rRMSE of 82 % and Model 1.2 resulted in an rRMSE of 52 %.

Biomass estimation based on SfM Volume

The best fitting tile edge length was found around 2 m (Figure 4.9). Using this tile edge length for further analysis the calculated volumes per segment varied between 286 and 3088 m^3 (Figure 4.10). The estimate c in Equation 4.3 (Model 2.1) was 1.14. The estimates d and f in Equation 4.4 (Model 2.2) were 0.28 and 1.38 respectively.

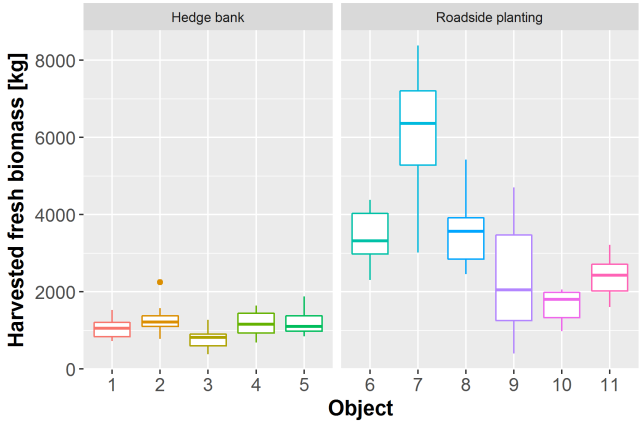

Figure 4.3: Harvested fresh biomass of eleven linear forest objects

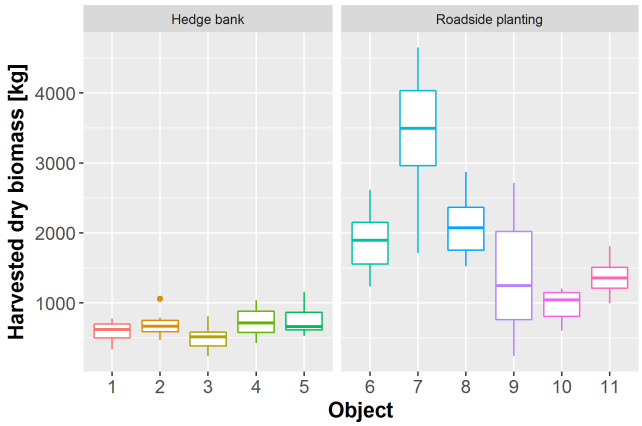

Figure 4.4: Harvested dry biomass of eleven linear forest objects

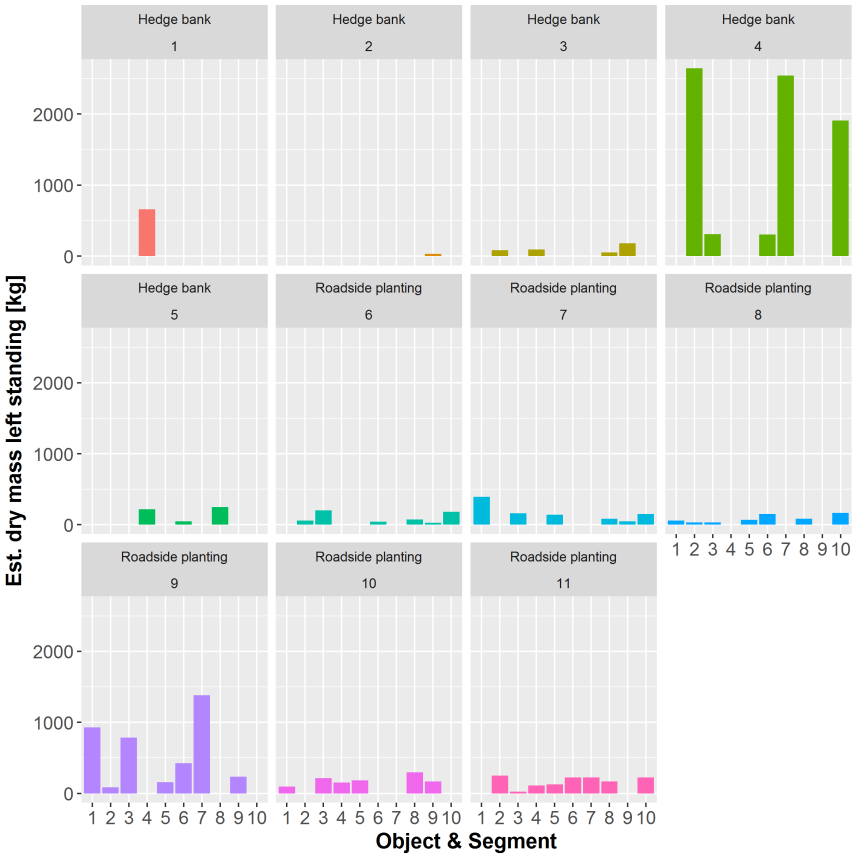

Figure 4.5: Estimated dry biomass of trees left standing. Estimations were calculated with equations from Zianis et al. (2005)

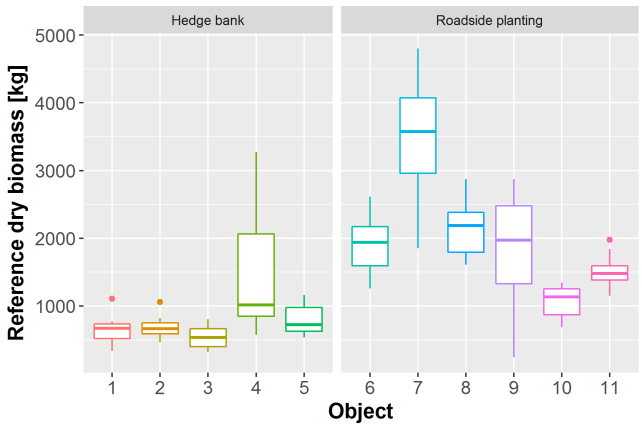

Figure 4.6: Reference dry biomass of eleven linear forest objects. Reference dry biomass is harvested dry biomass plus estimated dry biomass of trees left standing

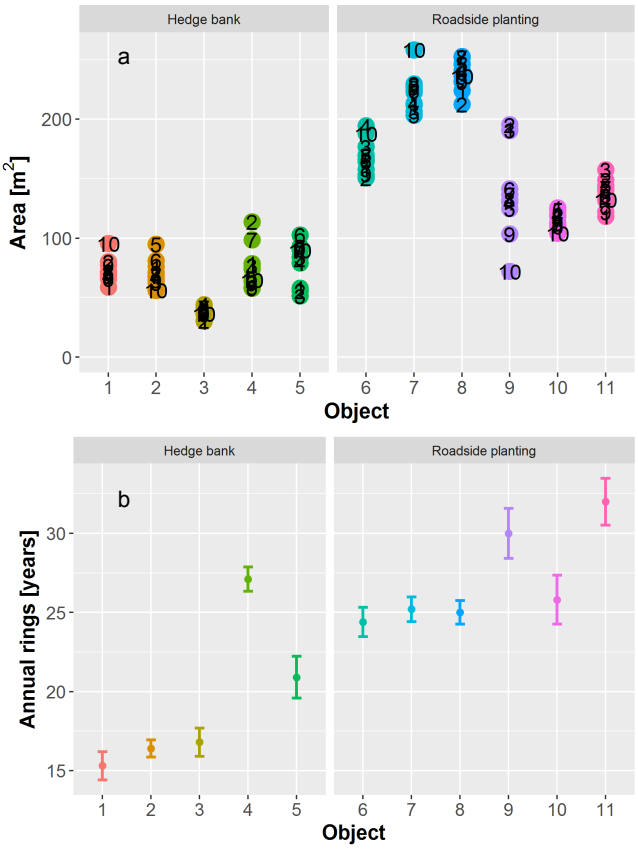

Figure 4.7: a) Canopy area of segments (Digitized in aerial images). b) Age of objects (Ascertained by annual ring counting). The points represent means and the error bars represent standard errors

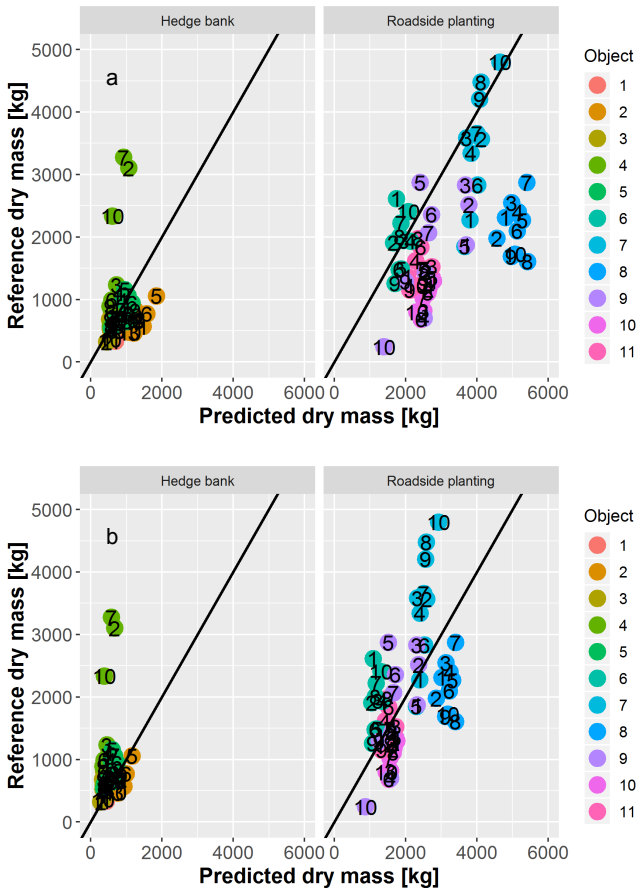

Figure 4.8: Predicted dry biomass (Equation 4.2) with two different prefactors (0.7 in a, 0.44 in b) vs. reference dry biomass. The line has a slope of 1 and presents an ideal fit

Table 4.2: Models with equations, parameters, rRMSE and CI_{SD} values

Model	Equation	rRMSE	CI_{SD} at 100 m
1.1	$\frac{dry\,mass_j}{kg} = 0.7 \cdot \frac{age_j}{year} \cdot \frac{canopy\,area_j}{m^2}$	82 %	
1.2	$\frac{dry\,mass_j}{kg} = 0.44 \cdot \frac{age_j}{year} \cdot \frac{canopy\,area_j}{m^2}$	52 %	82 %
2.1	$\frac{dry\,mass_j}{kg} = 1.14 \cdot \frac{SV_j}{m^3}$	31 %	33 %
2.2	$\frac{dry\,mass_j}{kg} = 0.28 \cdot \sum_{i=1}^{Number\,V\,in\,j} \left(\frac{V_i}{m^3}\right)^{1.38}$	30 %	

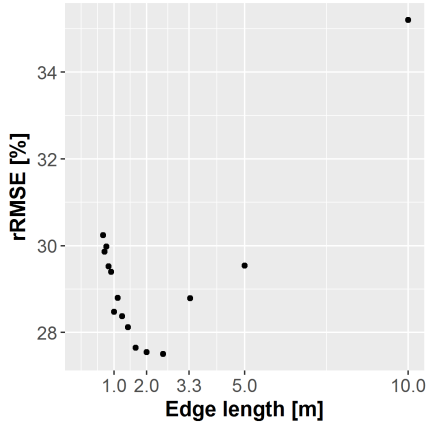

Figure 4.9: rRMSE of Model 1.1 with different tested tile edge lengths on a sub sample. Tested tile edge lengths were $10\,\mathrm{m}/n$ ($n = 1 \ldots 15$). The minimum rRMSE is roughly at 2 m

Model 2.1 resulted in an rRMSE of 31 % and Model 2.2 resulted in an rRMSE of 30 %. The data points of both models are presented in Figure 4.11. An overview of the models is presented in Table 4.2.

Different plot sizes

The data points of the larger plot sizes are presented in Figure 4.12. The rRMSE values of the three additional plot lengths of the area and age model were 47 % at 20 m, 43 % at 50 m and 42 % at 100 m. The rRMSE values of the three additional plot lengths of the SfM model were 27 % at 20 m, 19 % at 50 m and 16 % at 100 m. At the 100 m plot sizes the residuals of Model 1.2 resulted in a relative 95 % CI_{SD} of 82 % and the residuals of Model 2.1 resulted in a relative 95 % CI_{SD} 33 %. These rRMSE values are presented in Figure 4.13.

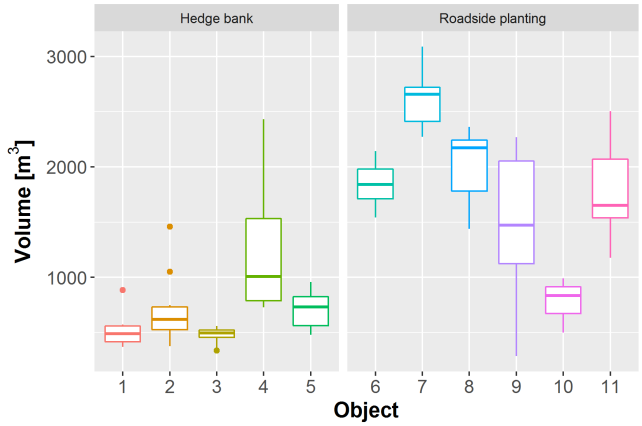

Figure 4.10: Volume calculations based on SfM of eleven linear forest objects

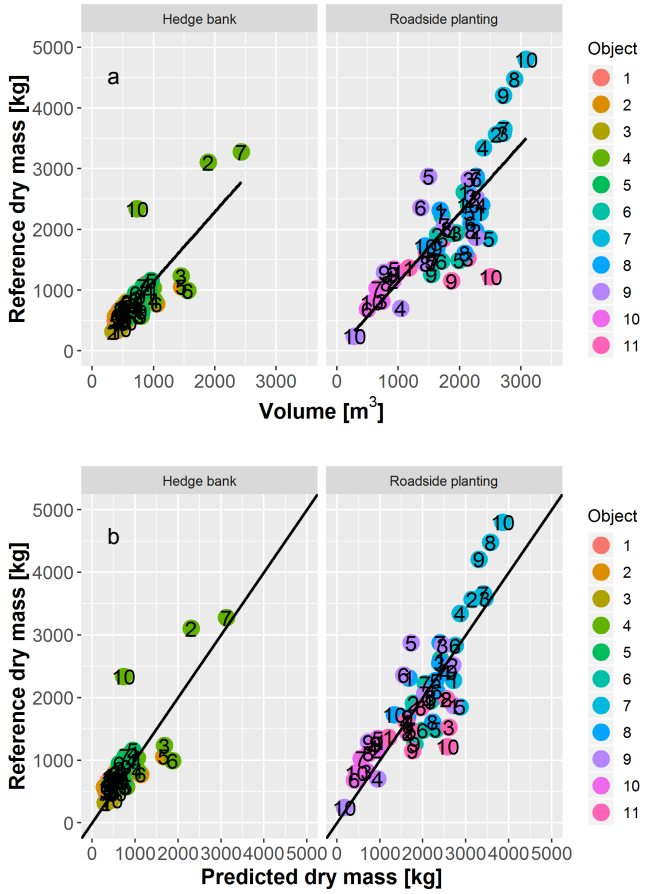

Figure 4.11: a) Volume vs. reference dry biomass (Equation 4.3 with a slope of $c = 1.14$). The line presents the linear model. b) Predicted dry biomass vs. reference dry biomass (Equation 4.4). The line has a slope of 1 and presents an ideal fit

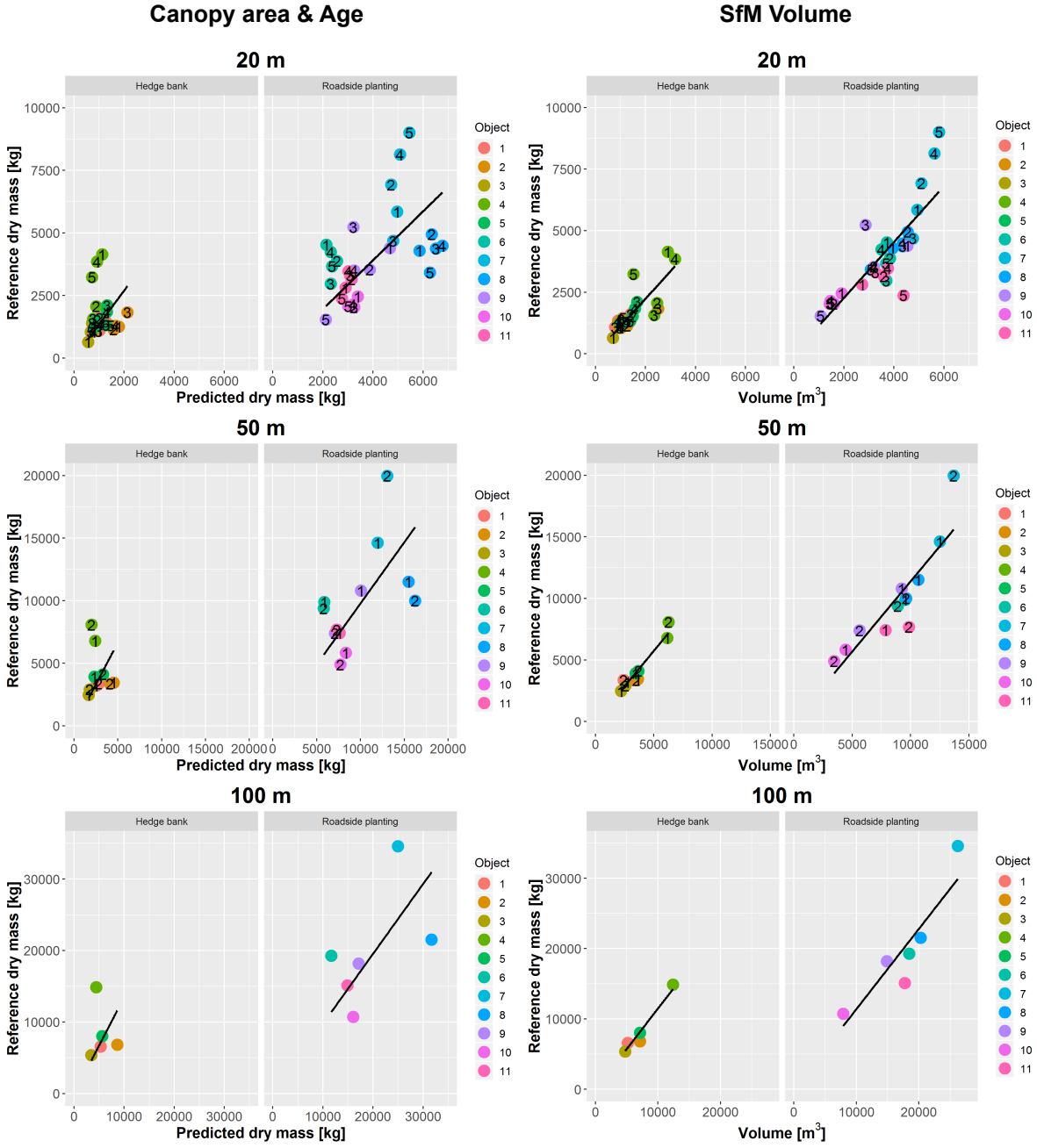

Figure 4.12: Predicted dry masses vs. reference dry masses and volumes vs. reference dry masses at different plot sizes.

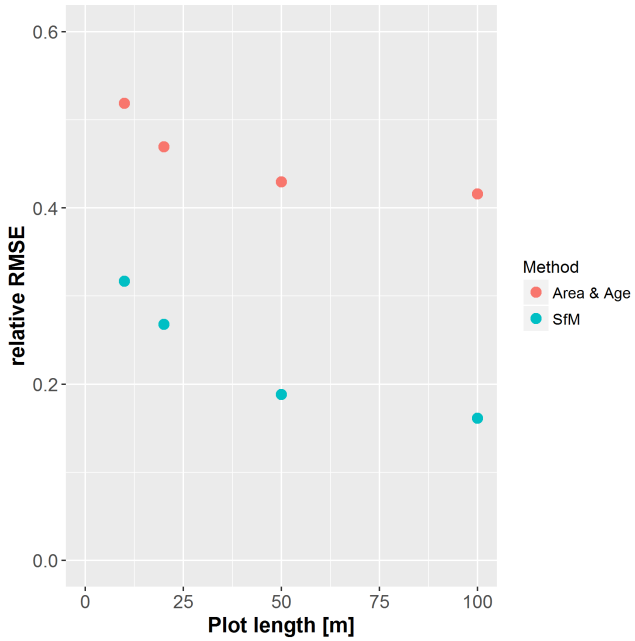

Figure 4.13: rRMSE of increased plot sizes

4.5 Discussion

Structure of hedge banks and roadside plantings

In the present study most hedge bank segments had smaller weights, canopy areas and volumes and were less old compared to the segments of the roadside plantings. The dry mass of the trees left standing per segment was around 9 % of the reference dry mass. However there were large differences between the objects.

Despite the small sample size of different objects the relationship between weight vs. canopy area times age and weight vs. volume appears to be similar in hedge banks and roadside plantings. Consequently the methods appear to be equally appropriate for both types of linear forest objects.

Accuracy of canopy area and age as predicting variables

Dry biomass estimation based on aerial images resulted in an rRMSE of 82 % (Model 1.1) and 52 % (Model 1.2). The spread of the data is the same in both models but the data points in Model 1.2 are further away from an ideal fit presented by a relation of 1:1. This difference explains the substantially different rRMSE values.

Model 1.1 and Model 1.2 are predicting almost the same dry biomass for every segment in a particular object. This can in part be explained by the fact that for all segments in a particular object the same age was assumed. This assumption is rationally since usually an entire object is felled at one time. Consequently, all segments of an object have the same age when regrowing.

At larger plot sizes this method resulted in an rRMSE of 42 %. The rRMSE values in literature for biomass estimation based on aerial images varied between 8 %

(Muukkonen and Heiskanen, 2007), 14 % (Ploton et al., 2012) and 40 % (Muukkonen and Heiskanen, 2005). However reference data in these studies were not gained by weighing but by less accurate techniques like allometric equations. So the rRMSE of these literature studies is not directly comparable to the present study since it is likely that a data set with a non-accurate reference method is worse than a data set with weighted reference values.

The present study could not confirm a prefactor of 0.7 as recommended by Seidel et al. (2015). The calculated prefactor of 0.44 in the present study was a lot smaller. In the present study the age of the objects were ascertained by annual ring counting after harvesting. For an absolute non-invasive method this needs to be done in a different way (e.g. exploration of historic data).

Accuracy of volume as predicting variable

Dry biomass estimation based on SfM volume resulted in an rRMSE of 30 % (Model 2.2). At larger plot sizes this method resulted in an rRMSE of 16 %. This rRMSE is in the range of the rRMSE from Miller et al. (2015) who have used SfM to calculate the volume of thirty bald single trees and received an rRMSE of 19 %. In Miller's study the single trees were photographed side-on all around. Dandois and Ellis (2010) have used SfM for biomass estimation at a small forest and received an rRMSE of 54 %. However, due to the large spatial scale they have used top-down photos only. Reference values were gained by allometric equations. Consequently the rRMSE values should be compared with caution here as well.

The rRMSE of Model 2.2 was not much lower than the rRMSE of Model 2.1. The additional parameter for volume height did not improve the model notably.

Comparison of accuracies

In the present study the rRMSE of the SfM volume approach was smaller than the rRMSE of the approach based on aerial images. It is not surprising that biomass is better described by volume than by canopy area since the canopy area in the optical images has no information about height. To substitute the height information age was added to the canopy area model (Model 1.1 and 1.2). However, the canopy area model was still worse than the volume model. Apparently, age is no equal substitution for height at the scale of the present study.

Ideal tile edge length for SfM

The best suitable tile edge length appeared to be roughly around 2 m. Larger and smaller tile edge lengths increased the rRMSE. Consequently a tile edge length of 2 m was used for SfM volume calculation.

Costs and time effort

SfM volume models appear to be more accurate than optical images for biomass estimation but the technical requirements for volume models are comparably high. Flying, point cloud generation and analysis is very time-consuming. Planning, preparation and flying for six objects took six working days with 8 h/d. Additionally the

calculation and processing of the point clouds took three weeks cpu time. This resulted approximately in 8 h for a UAV pilot and 8 h for a data analyst per 100 m. While the area and age approach only needs 2 h of a GIS analyst per 100 m. However, with some more experience and larger plot sizes the efficiency probably increases massively.

Different plot sizes

The rRMSE decreased considerably with increased plot sizes. This effect is probably in part due to decreased border errors. However another reason surly is that errors are averaged in larger plot sizes and consequently disguised.

Application in the field

Model 1.2 resulted in a relative 95 % CI_{SD} of 82 %. At a dry biomass of 10 t from typical 100 m hedge bank this CI_{SD} would result in a range between 2 and 18 t. Model 2.1 resulted in a relative 95 % CI_{SD} of 33 %. At a dry biomass of 10 t this CI_{SD} would result in a range between 7 and 13 t. The error of the models using aerial images is twice that high compared to the error of the volumes models. Consequently, the volume models should be preferred over models using optical images if smaller errors are essential.

Type of scales

In 2017 only a telescopic handler with a measurement resolution of 50 kg for weighing the two hedge banks (Object 1 and 2) was available. Fresh weights of the segments in these objects were between 700 and 2250 kg. The measurement resolution appears to be marginal at these weights. Consequently, mobile truck scales with a higher measurement resolution were used in 2018.

4.6 Conclusion

In the present study SfM volume models were calculated with leafy threes. Agisoft-Photoscan had problems with point cloud generation of leafless trees. These problems were probably due to lower colour contrasts between trees and soil. However so far the effect of the amount of leafs at a tree was not tested. Most likely the estimated volume of a tree in autumn with only a few leaves left is smaller than the estimated volume of the same tree in summer. This seasonal effect should be investigated in future.

In the present study a very expensive drone and camera setup was used. In a future study it should be tested if a more inexpensive setup with an off-the-shelf drone could achieve the same accuracy. Another approach in future could be the analysis of 3D satellite data. These data are quite expensive but cover large areas.

4.7 Acknowledgement

The European Innovation Partnerships and the Gesellschaft für Energie und Klimaschutz Schleswig-Holstein GmbH provided funding.

References

J. P. Dandois and E. C. Ellis. Remote Sensing of Vegetation Structure Using Computer Vision. *Remote Sensing*, 2(4):1157–1176, Apr. 2010. doi: 10.3390/rs2041157. URL http://www.mdpi.com/2072-4292/2/4/1157.

A. A. Dragulescu. xlsx: Read, write, format Excel 2007 and Excel 97/2000/XP/2003 files, 2014. URL http://CRAN.R-project.org/package=xlsx.

P. Hyde, R. Nelson, D. Kimes, and E. Levine. Exploring LiDAR-RaDAR synergy – predicting aboveground biomass in a southwestern ponderosa pine forest using LiDAR, SAR and InSAR. *Remote Sensing of Environment*, 106(1): 28–38, Jan. 2007. ISSN 0034-4257. doi: 10.1016/j.rse.2006.07.017. URL http://www.sciencedirect.com/science/article/pii/S0034425706002781.

E. Isensee, D. K. Stübig, and C. Lubkowitz. Bergung und Aufbereitung von Knick- und Schwachholz. *Landtechnik–Agricultural Engineering*, 55(5):346–347, 2000.

S. Lingner, E. Thiessen, K. Müller, and E. Hartung. Dry Biomass Estimation of Hedge Banks: Allometric Equation vs. Structure from Motion via Unmanned Aerial Vehicle. *Journal of Forest Science*, 64(4):149–156, 2018.

U. Mantau. *Holzrohstoffbilanz Deutschland, Entwicklungen und Szenarien des Holzaufkommens und der Holzverwendung 1987 bis 2015*. PhD thesis, Universität Hamburg, Hamburg, 2012.

J. Miller, J. Morgenroth, and C. Gomez. 3d modelling of individual trees using a handheld camera: Accuracy of height, diameter and volume estimates. *Urban Forestry & Urban Greening*, 14(4):932–940, 2015. ISSN 16188667. doi: 10.1016/j.ufug.2015.09.001. URL http://linkinghub.elsevier.com/retrieve/pii/S1618866715001223.

P. Muukkonen and J. Heiskanen. Estimating biomass for boreal forests using ASTER satellite data combined with standwise forest inventory data. *Remote Sensing of Environment*, 99(4):434–447, 2005. ISSN 0034-4257. doi: 10.1016/j.rse.2005.09.011. URL http://www.sciencedirect.com/science/article/pii/S0034425705003068.

P. Muukkonen and J. Heiskanen. Biomass estimation over a large area based on standwise forest inventory data and ASTER and MODIS satellite data: A possibility to verify carbon inventories. *Remote Sensing of Environment*, 107 (4):617–624, Apr. 2007. ISSN 00344257. doi: 10.1016/j.rse.2006.10.011. URL http://linkinghub.elsevier.com/retrieve/pii/S003442570600407X.

P. Ploton, R. Pélissier, C. Proisy, T. Flavenot, N. Barbier, S. N. Rai, and P. Couteron. Assessing aboveground tropical forest biomass using Google Earth canopy images. *Ecological Applications*, 22(3):993–1003, Apr. 2012. ISSN 1939-5582. doi: 10.1890/11-1606.1. URL http://onlinelibrary.wiley.com/doi/10.1890/11-1606.1/abstract.

S. C. Popescu, K. Zhao, A. Neuenschwander, and C. Lin. Satellite lidar vs. small footprint airborne lidar: Comparing the accuracy of aboveground biomass estimates and forest structure metrics at footprint level. *Remote Sensing of Environment*, 115 (11):2786–2797, Nov. 2011. ISSN 0034-4257. doi: 10.1016/j.rse.2011.01.026. URL http://www.sciencedirect.com/science/article/pii/S0034425711001325.

R Core Team. R: A Language and Environment for Statistical Computing, 2015. URL http://www.R-project.org/.

M. Segura, M. Kanninen, and D. Suárez. Allometric models for estimating aboveground biomass of shade trees and coffee bushes grown together. *Agroforestry Systems*, 68(2):143–150, June 2006. ISSN 0167-4366, 1572-9680. doi: 10.1007/s10457-006-9005-x. URL http://link.springer.com/article/10.1007/s10457-006-9005-x.

D. Seidel, G. Busch, B. Krause, C. Bade, C. Fessel, and C. Kleinn. Quantification of Biomass Production Potentials from Trees Outside Forests – A Case Study from Central Germany. *BioEnergy Research*, 8(3):1344–1351, Sept. 2015. ISSN 1939-1234, 1939-1242. doi: 10.1007/s12155-015-9596-z.

N. Snavely, S. M. Seitz, and R. Szeliski. Modeling the World from Internet Photo Collections. *International Journal of Computer Vision*, 80(2):189–210, Dec. 2007. ISSN 0920-5691, 1573-1405. doi: 10.1007/s11263-007-0107-3.

D. Turner, A. Lucieer, and C. Watson. An Automated Technique for Generating Georectified Mosaics from Ultra-High Resolution Unmanned Aerial Vehicle (UAV) Imagery, Based on Structure from Motion (SfM) Point Clouds. *Remote Sensing*, 4(12):1392–1410, May 2012. ISSN 2072-4292. doi: 10.3390/rs4051392. URL http://www.mdpi.com/2072-4292/4/5/1392/.

H. Wickham. *ggplot2: Elegant Graphics for Data Analysis*. Springer, New York, NY, 2009. ISBN 978-0-387-98140-6. URL http://ggplot2.org.

H. Wickham. The Split-Apply-Combine Strategy for Data Analysis. *Journal of Statistical Software*, 40(1):1–29, 2011. URL http://www.jstatsoft.org/v40/i01/.

S. Wood. Fast stable restricted maximum likelihood and marginal likelihood estimation of semiparametric generalized linear models. *Journal of the Royal Statistical Society*, 73(1):3–36, 2011.

D. Zianis, P. Muukkonen, R. Mäkipää, and M. Mencuccini. *Biomass and stem volume equations for tree species in Europe*. Number 4, 2005 in Silva Fennica monographs. Finnish Society of Forest Science, Finnish Forest Research Institute, Helsinki, Finland, 2005. ISBN 978-951-40-1983-8 978-951-40-1984-5. OCLC: ocm63646996.

5 Dry mass in linear forest objects: Structure from Motion sensitivity, Structure from Motion vs. expert, temporal pattern of growth and growth pattern vs. ecological value

Stefan Lingner, Eiko Thiessen, Eberhard Hartung

submitted to *Journal of Forest Science*

5.1 Abstract

The future demand for woody biomass could in part be supplied by harvested wood of existing hedge banks and roadside plantings. The estimation of this dry mass via different techniques was investigated in previous studies (Lingner et al., 2018a,b). Multiple questions arose during this process. These questions are worth to be investigated and discussed separately and are addressed in the present study. The topics investigated further in the present study are:

- Analysis of sensitivity (seasonal effect, amount of images, resolution of images)
- Structure from motion vs. experienced person
- Temporal pattern of growth
- Growth pattern vs. ecological value

The analysis of sensitivity showed that the seasonal effect had a small impact only. As a consequence flights can be performed both in summer or in autumn. The amount of images could be reduced, but not substantially in all objects. Consequently 600 images per 100 m linear forest object are recommended. A resolution of 6 megapixels is fine for the structure from motion application. In conclusion a consumer UAV is sufficient. The experts estimations were not generally better than the structure from motion estimations. Consequently for non-experts the structure from motion estimation is a good solution. The growth rate was not lineally, but sigmoidally related to age. This growth rate can be taken into account for a higher dry mass performance. The ecological value was not related to growth rate. In conclusion a high ecological value and a high dry mass yield is no conflict of interests.

5.2 Introduction

It was shown in the previous studies that structure from motion (SfM) can be used for biomass estimation at hedge banks and roadside plantings (Lingner et al., 2018a,b). However multiple questions arose during the process of investigation. These questions are addressed below.

Analysis of sensitivity

Seasonal effect

In the previous studies (Lingner et al., 2018a,b) SfM volume models were calculated with leafy threes. The program AgisoftPhotoscan had problems with point cloud generation of leafless trees. These problems were probably due to little colour contrasts between trees and soil. However so far the effect of the amount of leafs at a tree was not tested. Most likely the estimated volume of a tree in autumn with only a few leaves left is smaller than the estimated volume of the same tree in summer. In the present study SfM models of hedge banks with a lot leaves (summer) are compared to SfM models with few leaves (autumn).

Amount of images

It is likely that there were more images taken than necessary in the previous studies (Lingner et al., 2018a,b). The octocopter flew on each side of the 100 m hedge banks at four different heights. The ends of the flight routes always were a little beyond the end of the objects. Consequently the total flown distance usually was around 1200 m. About every two metres an image was taken. This resulted in approximately 600 images per object. In the present study the minimum necessary amount of images was investigated.

Resolution of images

The camera used in the previous studies (Lingner et al., 2018a,b) had a resolution of 24 megapixels. This are more pixels than a camera of a state of the art consumer unmanned aerial vehicle (UAV) has. One of the most common UAV is the DJI Phantom. The current version of the DJI Phantom (DJI Phantom 4) has 12 megapixels. In the present study it was tested whether SfM models of hedge banks are possible with a lower resolution camera as well.

SfM vs. experienced person

In the previous studies (Lingner et al., 2018a,b) it was shown that SfM models can be used to predict dry mass at linear forest objects. In the present study this prediction accuracy of SfM models is compared to predictions made by experienced persons.

Temporal pattern of growth

The previous paper showed that dry mass yield can roughly be estimated by canopy area times age (Lingner et al., 2018a). This resulted in the question whether age is linearly related to the dry mass increment. The answer to this question could help finding the ideal time of harvest to maximise dry mass yield.

Growth pattern vs. ecological value

The hedge banks investigated in the previous studies (Lingner et al., 2018a,b) had diverse species compositions. These different species compositions lead to different ecological values. Consequently the question occurred whether a high ecological value and a high dry mass yield are conflicting interests. In the present study it was tested whether dry mass yield per area and year is related to the ecological value of the object.

5.3 Methods

Data acquisition

Data for the present study were sampled in 2016, 2017 and 2018 at eleven linear forest objects in Schleswig-Holstein, Germany. These objects consisted of five different hedge banks and six roadside plantings. A representative length of 100 m was selected for each object. Hedge banks and roadside plantings were selected to differ in species

composition, width, alignment and age. The species compositions covered the most dominant types of linear forest objects in Schleswig-Holstein. These diverse objects were sampled that results have a broad scope of application for different linear forest objects in Schleswig-Holstein.

To gain reference data all shrubs and trees of each segment were felled, chopped to wood-chips and weighed segment-wise. From each segment three samples of wood-chips (approx. 5 litres each) were taken. These samples were dried at 103° C to constant weight according to DIN 52183 for dry mass content estimation. Thus the dry mass of every segment could be estimated.

Usually not all trees are felled in hedge banks and roadside plantings. Some trees are left standing for ecological reasons. However these trees were part of the SfM-volume models and aerial images. Consequently the dry masses of the trees left standing were estimated based on species-specific allometric equations provided by Zianis et al. (2005) and added to the harvested dry masses to gain the total reference dry masses. For more details on the experimental design see previous papers (Lingner et al., 2018a,b).

Not all objects were considered for all of the following analyses. For the analysis of sensitivity three hedge banks were considered. For the analysis of SfM vs. experienced person three hedge banks and three roadside plantings were considered. For the remaining analyses all objects were considered.

Analysis of sensitivity

Seasonal effect

SfM models of three hedge banks were generated with images taken both in July 2017 (summer) and in November (autumn) 2017. Volumes for each of the hedge banks' segments were calculated twice. The first calculation based on the summer model and the second calculation based on the autumn model. The volumes of both models' segments were compared.

Amount of images

The amount of iamges of three hedge banks was reduced step by step. The original amount of images was around 600 at each of the three objects. 100 images were randomly deleted in each turn. This reduction was performed as long as the program AgisoftPhotoscan was able to generate an SfM model with these images. If the resulting point cloud did not cover the entire 100 m the process was considered to have generally failed. The overlap between images estimated by AgisoftPhotoscan of the model with the fewest images possible was recorded. The segments' volumes of the models generated with fewer images were compared with the segments' volumes of the original model.

Resolution of images

The images' resolution of three hedge banks was downsampled from 24 megapixels to a resolution of 6 megapixels. This process was performed in R based on mean values. A resolution of 6 megapixels results in a pixel size of 12 mm × 12 mm at

a distance of 30 m. One SfM model from the original sized images and one model from the downsampled images were generated per object. Afterwards the segments' volumes of the models generated with the downsampled images were compared with the segments' volumes of the original models.

SfM vs. experienced person

The dry mass yield of three hedge banks and three roadside plantings were estimated by an experienced person. The expert for the hedge banks was an employee of the agricultural contracting business contracted to harvest the hedge banks. This expert estimated in cubic metres. The expert for the roadside plantings was the owner of the contracting business contracted to harvest the roadside plantings. This expert estimated in dry mass. The experts' estimations were compared to the reference dry masses. The relative root mean square error (rRMSE) of these predictions was compared to the rRMSE of the predictions by the SfM models. For the rRMSE calculation the data from the experts and the volumes were treated in the same way. First a statistical model was build for calibration. This model had the reference dry masses as depended variable and the experts estimations or the volumes as independent variable. Based on this model the rRMSE was calculated for model validation.

Temporal pattern of growth

Two statistical models were built to address the temporal growth pattern of eleven linear forest objects. In the first model dry mass is explained by canopy area times age (linear model, LM). In the second model dry mass is explained by canopy area times age and an additional smooth function for age (additive model, GAM). No intercept was allowed in these models. The residuals of both models were plotted vs. age for pattern recognition. The residuals of a statistical model is the part of the variation, that is not explained yet. Plotting these residuals against a variable that is or is not in the model helps detecting unexplained patterns (Zuur et al., 2009). The Akaike information criterion (AIC) of both models was compared additionally. The AIC is a goodness of fit estimator of the relative quality of the statistical model. Statistics and graphics were performed in R (R Core Team, 2015) implementing the mgcv package (Wood, 2011) and the ggplot package (Wickham, 2009).

Growth pattern vs. ecological value

To investigate the effect of ecological value on growth per area and year the residuals of the previous GAM were plotted against the ecological value of the object. The Institute for Natural Resource Conservation of the University of Kiel calculated an ecological value for every object based on species composition and margin quality (unpublished data).

5.4 Results

Analysis of sensitivity

Seasonal effect

The hedge banks had considerably less leafs in November compared to July (Figure 5.1). The rRMSE between the volumes from July and the volumes from November was 11.5 %. The data points are presented in Figure 5.2. Volumes from both seasons are mainly close to a 1:1 ratio. However some of the calculated volumes of hedge bank 1 and 3 appear to be a little smaller in November compared to July.

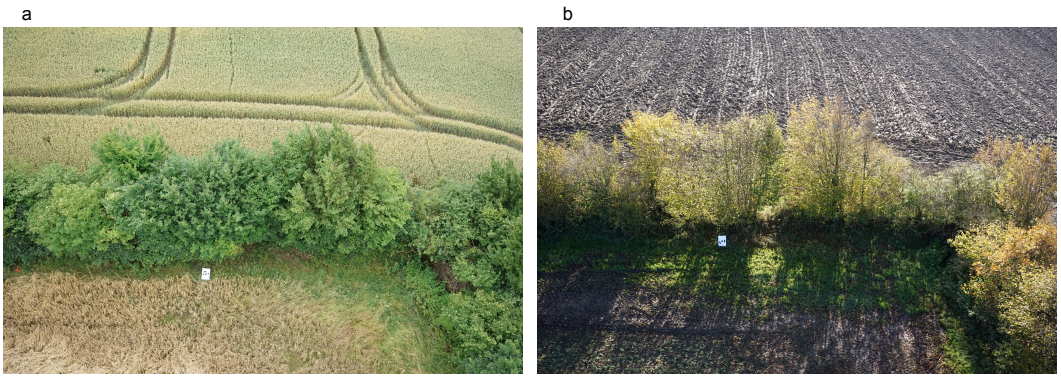

Figure 5.1: Hedge bank 1 in July 2017 (a) and in November 2017 (b) with considerably less leaves in November

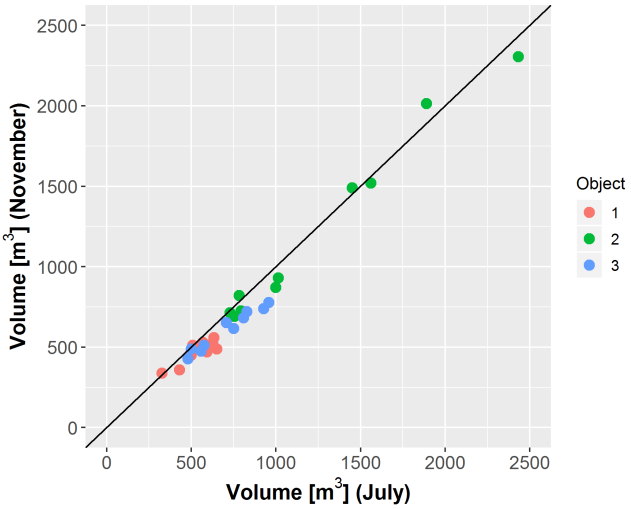

Figure 5.2: Segments' volumes in summer compared to segments' volumes in autumn. The line represents an 1:1 ratio

Amount of images

The segments' volumes of the models generated with fewer images are compared to the segments' volumes of the original model in Figure 5.3, Figure 5.5 and Figure 5.7. SfM models with fewer images than presented could not be generated. Images of the objects are presented in Figure 5.4, Figure 5.6 and Figure 5.8. The minimum amount of images possible in Object 1, 2 and 3 were 300, 500 and 200 respectively. The overlap of the images was still above 90 % in these models. Volumes from all models that did not generally fail were close to a 1:1 ratio. There is no pattern visible that this ratio is worse with fewer images. As long as the program AgisoftPhotoscan was able to generate an SfM model the volumes are comparable to the model with all images.

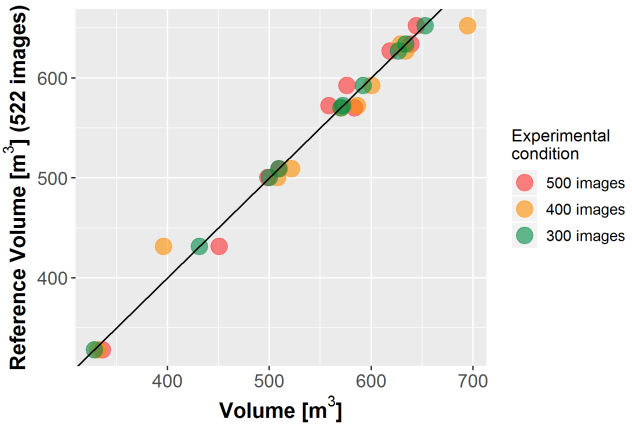

Figure 5.3: Object 1. The segments' volumes of the models generated with fewer images compared to the segments' volumes of the original model. The line represents an 1:1 ratio

Figure 5.4: Image of Object 1

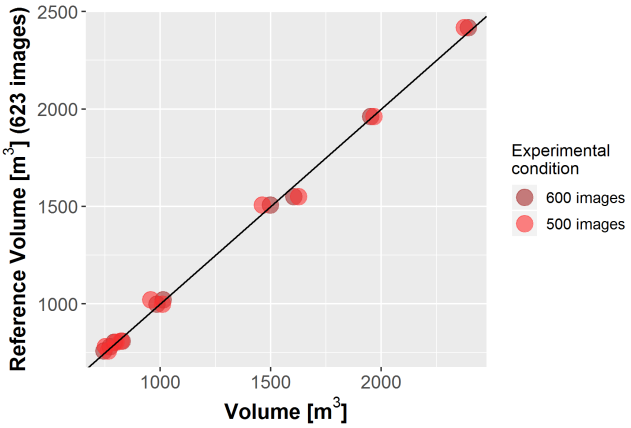

Figure 5.5: Object 2. The segments' volumes of the models generated with fewer images compared to the segments' volumes of the original model. The line represents an 1:1 ratio

Figure 5.6: Image of Object 2

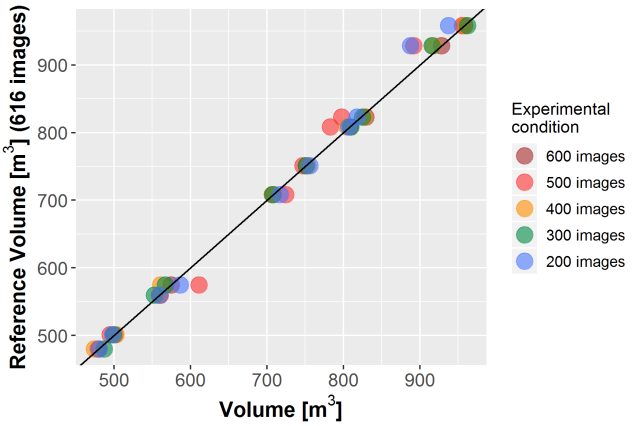

Figure 5.7: Object 3. The segments' volumes of the models generated with fewer images compared to the segments' volumes of the original model. The line represents an 1:1 ratio

Figure 5.8: Image of Object 3

Resolution of images

The segments' volumes generated with the downsampled images are compared to the segments' volumes of the original models in Figure 5.9. The rRMSE was at 5.3 %. Volumes from all models were close to a 1:1 ratio. There is no pattern visible that volumes derived from a resolution of 6 megapixels produce smaller or larger volumes compared to models derived from 24 megapixels.

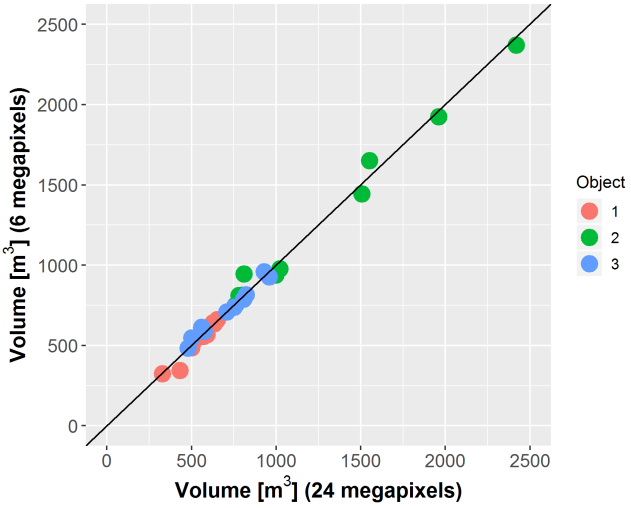

Figure 5.9: The segments' volumes generated with the downsampled images compared to the segments' volumes of the original model. The line represents an 1:1 ratio

SfM vs. experienced person

The predictions by the expert for the dry masses of the hedge banks resulted in an rRMSE of 59 % (Figure 5.10a). The predictions made by the SfM model resulted in an rRMSE of 42 % (Figure 5.10b). The predictions by the expert are linearly related with the reference dry masses of Object 1. However the predictions are poorly linearly related with the reference dry masses of Object 2 and 3 while the worst fit is with the reference dry masses of Object 2. The SfM volumes are linearly related with the reference dry masses of Object 1 and 3. However the SfM volumes are poorly linearly related with some of the reference dry masses of Object 2. Object 2 was worst related with both the experts' estimation and with the SfM volumes. The large amount of mismatch might be due to a large number of dead trees in this object.

The predictions by the expert for the roadside plantings resulted in an rRMSE of 30 % (Figure 5.11a). The predictions made by the SfM model resulted in an rRMSE of 34 % (Figure 5.11b). The predictions by the expert are equally linearly related with the reference dry masses of all objects. The SfM volumes are linearly related with the reference dry masses of Object 5. However the SfM volumes are less linearly related with the reference dry masses of Object 4 and 6. At the time of writing the reasons for this mismatch are obscure to the author.

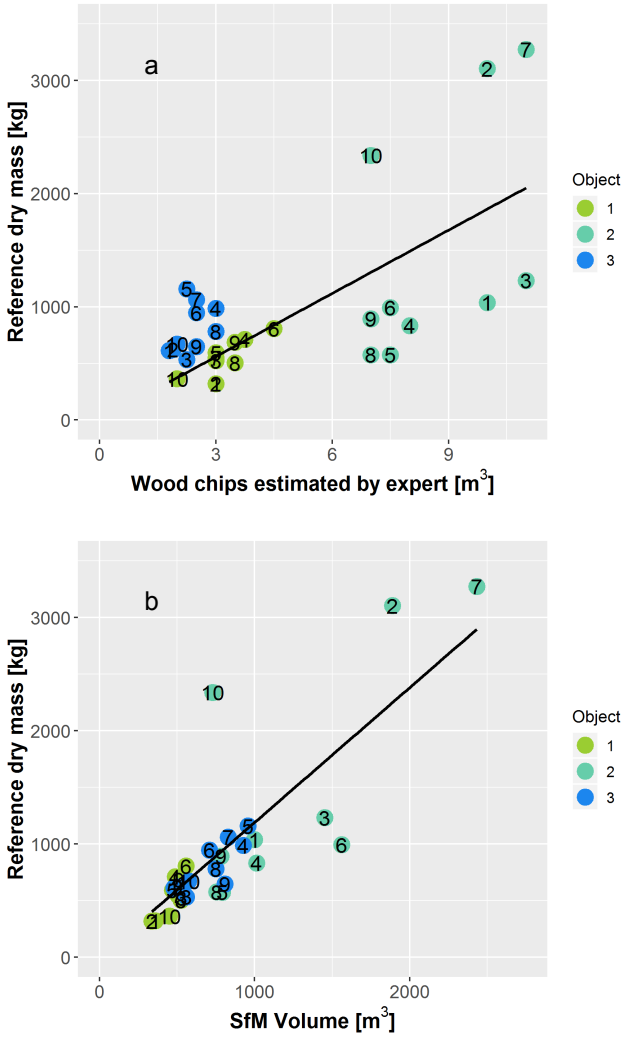

Figure 5.10: Dry mass estimations made by an expert (a) compared to the estimations of an SfM model (b) at hedge banks. This expert estimated in cubic metres. The line represents a linear model

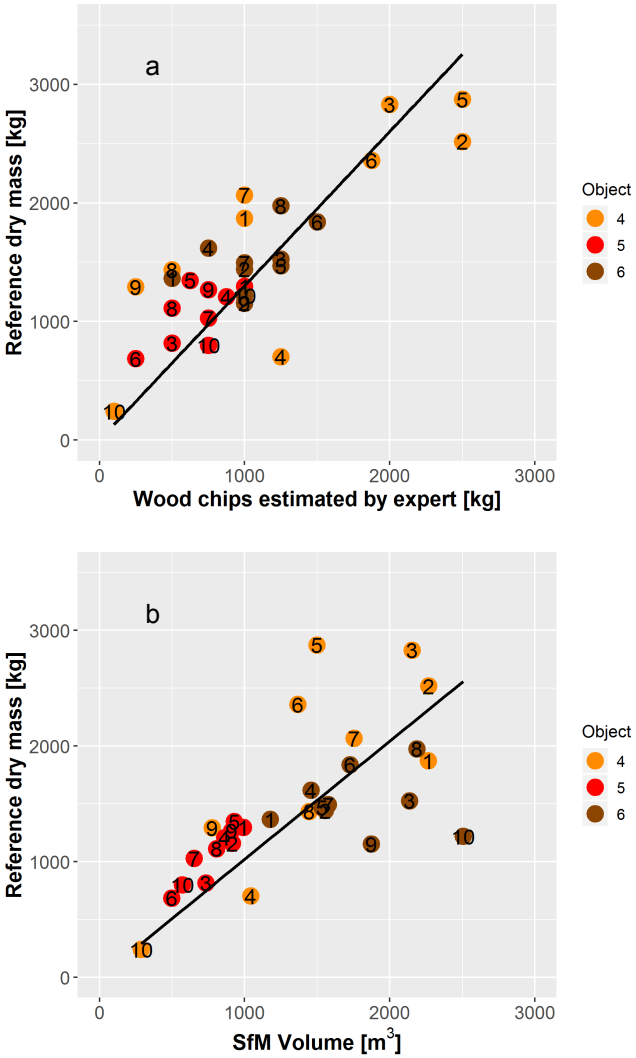

Figure 5.11: Dry mass estimations made by an expert (a) compared to the estimations of an SfM model (b) at roadside plantings. This expert estimated in kg. The line represents a linear model

Temporal pattern of growth

Canopy area times age (LM, $F_{1,\ 109} = 477$, $p < 0.0001$) was significant in the LM. Data points are plotted in Figure 5.12a and residuals vs. age are plotted in Figure 5.12b. In the LM there is a strong pattern visible that younger objects have positive residuals and older objects have negative residuals. The tipping point is at around 25 years. The vegetation has a strong growth rate at younger years, but after around 25 years the organisms start to compete for resources. As a consequence the growth rate decreases.

Both canopy area times age (GAM, $F_{1,\ 105.4} = 939$, $p < 0.0001$) and the smooth function for age (GAM, $F_{3.6,\ 105.4} = 25$, $p < 0.0001$) were significant in the GAM. The

smooth function is presented in Figure 5.13. Data points are plotted in Figure 5.14a and residuals vs. age are plotted in Figure 5.14b. The pattern visible in the LM has vanished in the GAM. The AIC for the LM was 1775 and the AIC for the GAM was 1710.

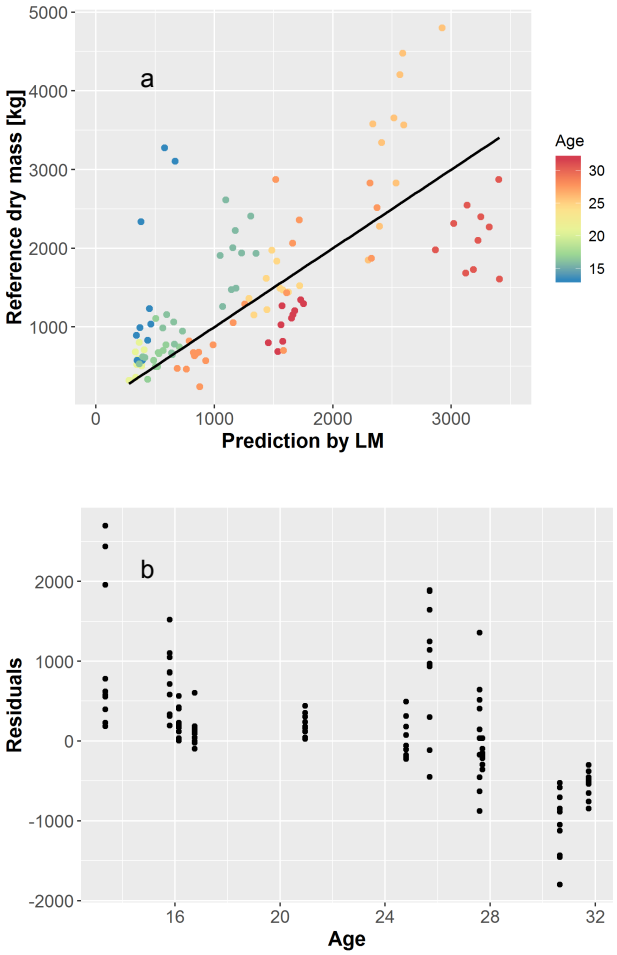

Figure 5.12: Data points (a) and residuals against age (b) of the linear model

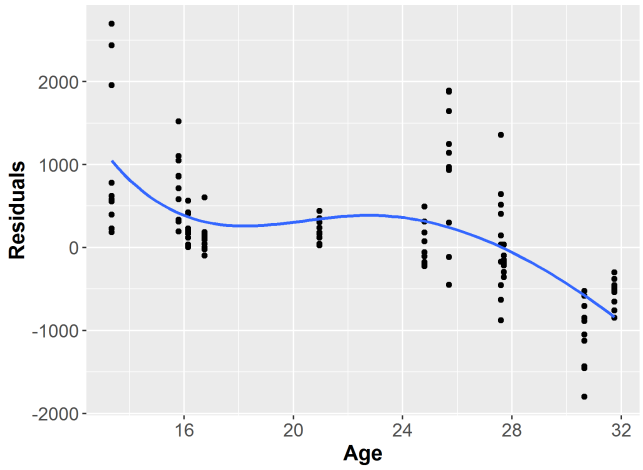

Figure 5.13: Smooth function for age in the additive model

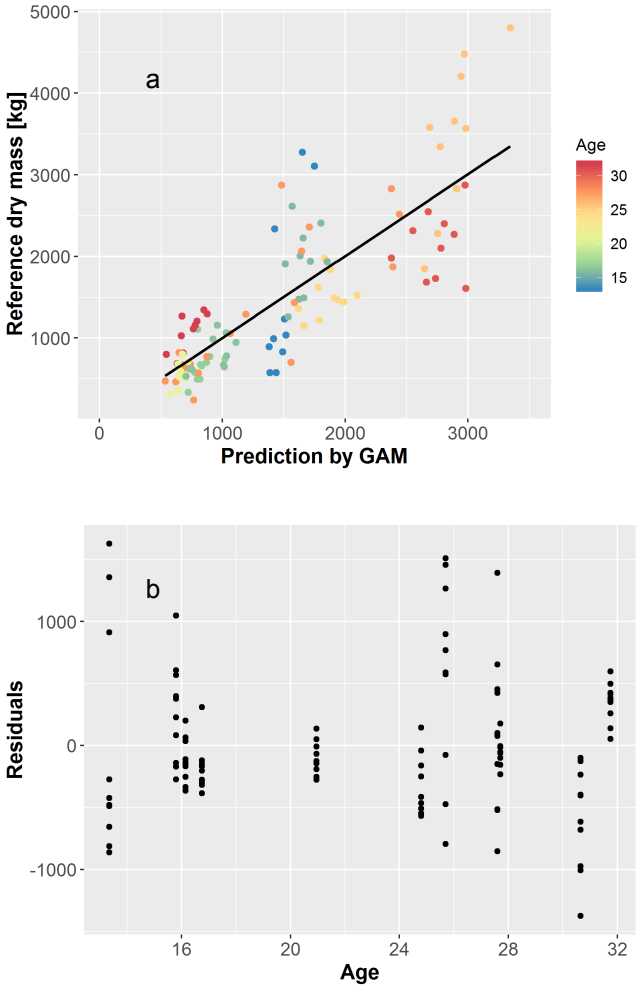

Figure 5.14: Data points (a) and residuals against age (b) of the additive model

Growth pattern vs. ecological value

Residuals of the GAM plotted against ecological values are presented in Figure 5.15. No directional pattern is visible in the residuals.

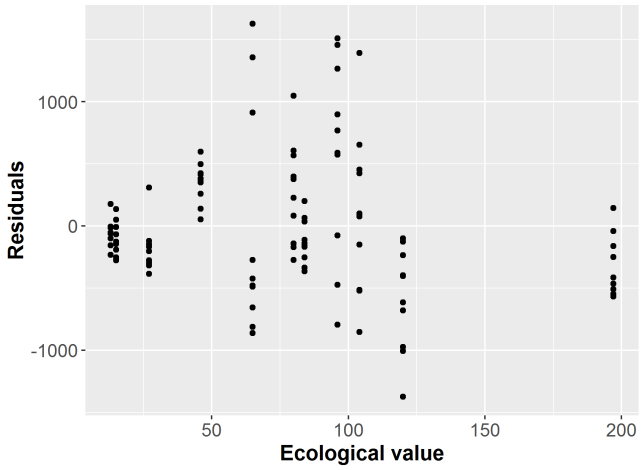

Figure 5.15: Residuals of the GAM plotted against ecological values

5.5 Discussion

Data acquisition

Due to the diverse properties and species compositions of the objects sampled the results of this study are likely to be applicable to all linear forest objects in Schleswig-Holstein. The segments sampled were 10 m long. These plot sizes are comparably small for real life applications. However this size was chosen to get a very detailed stocktaking of the objects. It was still possible to group plots for larger plot sizes afterwards like done in Lingner et al. (2018b).

Analysis of sensitivity

Seasonal effect

Especially at smaller values the volumes appear to be a little larger in summer than in autumn. However, the prediction of biomass in hedge banks with SfM resulted in an rRMSE of around 30 %. Consequently an error of 11.5 % due to a seasonal effect appears to be negligible. Unfortunately no literature is published about this topic at the time of writing. So values could not be compared.

Amount of images

The SfM models could be generated with fewer images as has been done in Lingner et al. (2018a,b). However Object 2 still needed 500 of 600 images. Consequently 600 images per 100 m linear object appears to be a solid recommendation for future applications. As long as the models could be generated the volumes were comparable

to the volumes of the models with all images. The amount of images necessary surly in part depends on structures recognisable by the algorithm of AgisoftPhotoscan.

AgisoftPhotoscan is the most common fee requiring program for SfM applications. There is no reason to assume that other programs would perform better with the given images.

Resolution of images

The volumes of the models from the downsampled images are comparable to the volumes of the original models. The rRMSE of 5.3 % is negligible. Consequently SfM models of linear forest objects should be possible with a consumer UAV as well. In particular since the tested resolution (6 megapixels) is half of the resolution of a state of a the art consumer UAV.

SfM vs. experienced person

The predictions made by the expert at the hedge banks was a lot worse than the predictions made by the expert at the roadside plantings. The major reason for this difference probably is the different ability or experience of these two persons.

The hedge bank 3 was completely underestimated by the expert. The reason for this underestimation might be the species composition of this hedge bank. A large part of the species in this hedge bank were shrubs like blackthorn (*Prunus spinosa*). This high proportion of shrubs might have influenced the expert to guess less.

The SfM model was a slightly worse (4 %) predictor compared to the expert at the roadside plantings but was a better predictor compared to the expert at the hedge banks. Summing up the SfM model appears to be comparable to human experts. However it can be applied without experience.

Temporal pattern of growth

The residuals of the LM showed a clear pattern in relation to age. This pattern was removed by implementing a smooth function for age in the GAM. The AIC was lower in the GAM, which indicates a better fit.

The smooth function of the GAM indicates that there is a small growth rate in the first 15 years. After this period the growth rate maximises until approximately 25 years and decreases again afterwards. This shape of the curve does not surprise since trees are expected to have a sigmoidal growth curve like all organisms (West, 1987; Weiner and Thomas, 2001). The growth is finally constrained by limited recourses like light.

These results indicate that linear forest objects should not be harvested before 25 years of growth to maximise wood yield. Plus, even if the growth rate declines the wood yield per working hour of harvesting still increases. Still an early harvest should be considered for legal and ecological reasons or to minimise the shadow on adjacent agricultural areas.

Growth pattern vs. ecological value

There is no pattern visible in Figure 5.15 that would indicate that dry mass yield per area and age depends on the ecological value. In conclusion there is no reason not to support a species composition with a high ecological value when aiming for a high dry mass yield.

References

S. Lingner, E. Thiessen, and E. Hartung. Biomass estimation in linear forest objects: Structure from motion vs. aerial images. *unpublished*, 2018a.

S. Lingner, E. Thiessen, K. Müller, and E. Hartung. Dry Biomass Estimation of Hedge Banks: Allometric Equation vs. Structure from Motion via Unmanned Aerial Vehicle. *Journal of Forest Science*, 64(4):149–156, 2018b.

R Core Team. R: A Language and Environment for Statistical Computing, 2015. URL `http://www.R-project.org/`.

J. Weiner and S. C. Thomas. The Nature of Tree Growth and the "Age-related decline in forest productivity". *Oikos*, 94(2):374–376, 2001. ISSN 0030-1299. URL `https://www.jstor.org/stable/3547583`.

P. W. West. A Model for Biomass Growth of Individual Trees in Forest Monoculture. *Annals of Botany*, 60(5):571–577, Nov. 1987. ISSN 1095-8290, 0305-7364. doi: 10.1093/oxfordjournals.aob.a087480. URL `https://academic.oup.com/aob/article/127480/A`.

H. Wickham. *ggplot2: Elegant Graphics for Data Analysis*. Springer, New York, NY, 2009. ISBN 978-0-387-98140-6. URL `http://ggplot2.org`.

S. Wood. Fast stable restricted maximum likelihood and marginal likelihood estimation of semiparametric generalized linear models. *Journal of the Royal Statistical Society*, 73(1):3–36, 2011.

D. Zianis, P. Muukkonen, R. Mäkipää, and M. Mencuccini. *Biomass and stem volume equations for tree species in Europe*. Number 4, 2005 in Silva Fennica monographs. Finnish Society of Forest Science, Finnish Forest Research Institute, Helsinki, Finland, 2005. ISBN 978-951-40-1983-8 978-951-40-1984-5. OCLC: ocm63646996.

A. Zuur, E. Ieno, N. Walker, A. Saveliev, and G. Smith. *Mixed Effects Models and Extensions in Ecology with R*. Springer New York, 2009.

6 Generel Discussion

Aim and content

This general discussion covers experiences gained, decisions made and recommendations for the future that are worth to be discussed generally for all previous chapters. The discussion is split into the discussion of the methods and the discussion of the results.

The objects sampled are discussed as the first topic in the methods' section. Samples always are the base for any statistical analysis and consequently are worth to be discussed. At second the level of detail possible in SfM models is discussed. During the process of investigation a lot of experience was gained regarding the level of detail possible at SfM applications of trees. An alternative approach to SfM would have been the utilization of Lidar. This topic is discussed in the methods' section as well. The next part of the methods' section is the discussion of the reference samples. These samples were taken to estimate dry mass content and calorific values. The last part of the methods' section is the discussion of the plot sizes. It was shown that the errors decreased notably with increased plot sizes. Consequently the chosen size of the plots is worth to be discussed.

The first part of the results' section is the discussion of the dry mass and SfM volume relationship. Lingner et al. (2018c) and Lingner et al. (2018b) calculated different slopes between SfM volume and dry mass. Consequently this value is worth to be discussed. The second part covers the growth per area and year. Lingner et al. (2018c) estimated a growth rate that was notably different to Seidel et al. (2015) and hence needs to be discussed. The last two parts cover further applications possible and future applications imaginable.

Discussion of Methods

Object samples

So far the current project lasted two seasons (2016/2017 and 2017/2018). In every season three hedge banks and three roadside plantings were intensively investigated. SfM models at different seasons were generated. The species of every shoot higher than one metre was distinguished. All trees and shrubs were felled, chopped to woodchips and weighed segment-wise. This resulted in 12 objects intensively investigated. Unfortunately the marks of one hedge bank were accidentally removed by a farmer during the first season. Consequently only 11 objects (110 segments) could be used for most of the analyses. However the sample size turned out to be sufficient for the aims of the study.

Increasing the sample size per year would have necessarily resulted in a less detailed survey of the objects. However the aim of the project particularly was to collect

detailed information. Otherwise the classification of the ecological value would not have been possible.

Sampled hedge banks and roadside plantings had diverse species compositions. Some of the hedge banks had a large proportion of blackthorn (*Prunus spinosa*) other objects were dominated by willow (genus *Salix*), sycamore (*Acer pseudoplatanus*) or common hornbeam (*Carpinus betulus*). Most frequent counted shoots of all segments were blackthorn, fly honeysuckle (*Lonicera xylosteum*) and common hazel (*Corylus avellana*). These species compositions are a good representation of linear forest objects in Schleswig-Holstein, Germany (Eigner, 1982). As a consequence the results of this study are likely to be applicable to all linear forest objects in Schleswig-Holstein. However the results might me less applicable to linear forest objects outside of Schleswig-Holstein.

Level of detail in SfM models

3D models of single trees or entire forest objects can be more or less detailed. A broad model only shows the outline of the object, while a more detailed 3D model shows stems and a very detailed model shows smaller branches as well. Miller et al. (2015) has constructed very detailed 3D models of small stand-alone trees using SfM. It was tried to copy this process at hedge banks for the previous studies. However it had to be realized that generating detailed models of trees using SfM is possible at very specific conditions only. SfM bases on computer vision (Snavely et al., 2007; Turner et al., 2012). Consequently SfM works only if the algorithm is able to distinguish objects in the photos. During the investigations for the previous papers (Lingner et al., 2018b,c) it was experienced that for a detailed model of a tree the following conditions need to be met:

- The tree must stand alone. When the algorithm is fed with hundreds of photos with thousands of small branches of hundreds of trees the algorithm can't distinguish the trees, let alone the branches.
- The background must not be soil when the tree is without leafs. When the background of the photos has the same colour as the object that is supposed to be modelled the algorithm can't distinguish the object.
- All parts of the tree need to be visible and not masked by other parts. When there are parts of the tree that can't be photographed all around the surface of the resulting model has missing parts. In this case it is hard to distinguish two adjacent branches. This implies the risk that two or more small branches are taken for one thick stem. This error would result in an enormous error at volume calculations.

None of these conditions were met at the hedge banks or roadside planting. It consequently failed when trying to model a linear forest object detailedly. It was not possible to model the branches of a tree since the algorithm could not distinguish them. Yet not all stems of a linear forest object could be modelled since they masked each other. Plus bunches of smaller branches or shrubs were taken for stems. Consequently it was decided to follow the only practical way, which was an enclosing model of a

leafy object. Against the backdrop of the results in the previous papers this decision appears to be reasonable.

Lidar

An alternative option to create detailed 3D models of trees is the utilization of Lidar (Dittmann et al., 2017). This method was considered as well. The advantage of Lidar is that object distinction does not rely on computer vision. Similar object shapes and similar colours are no problem for Lidar. However the laser beams can't penetrate tree stems neither. Consequently the trees would still mask each other. Dominik Seidel from the University of Göttingen is an expert of Lidar applications at trees (Seidel et al., 2011a,b, 2012). He had tried to scan and model hedge banks prior to the present studies. He as well recommended via personal communication that hedge banks are too dense for Lidar applications. Consequently it was decided to stick to SfM.

Reference samples

Relative dry masses and calorific values were determined for every segment. From each segment three samples of wood-chips (approx. 5 litres each) were taken. At each sample dry mas was determined according to DIN 52183 and calorific value was determined according to DIN 51900.

However neither relative dry mass, nor calorific value could be related to the species composition in the segment (unpublished data). For example, it could be stated that segments with a high proportion of shrubs like blackthorn (*Prunus spinosa*) would have a lower calorific value due to a larger bark content. However this hypothesis could not be confirmed.

One reason for this result could be the method of sampling. A sample of 1.5 kg of a segment with 3000 kg of wood chips represents a proportion of 0.05 %. Three of these samples only represents 0.15 %. The proportion of the samples might be too small to represent an entire segment. For detailed results the sample size probably should be rather around 30 than three. Without increasing the resources a larger sample size would have resulted in fewer objects covered. However the aim of the current project was rather to cover a large diversity of linear forest objects than to investigate only one object very detailed.

Plot size

The rRMSE decreases notably at larger plot sizes as shown in (Lingner et al., 2018b). As discussed the reason for this effect is probably both due to decreased border errors and due to averaged errors. However the plot size in in the previous studies was limited by several restrictions and consequently set to a length of 10 m. The two major restrictions were:

- Weighing the dry weight of one segment should still be feasible and not way too much effort. Larger plot sizes would have resulted in more truckloads to weigh.

- Shoots higher than one metre of all trees and shrubs were counted and distinguished. At larger plot sizes this data collection would have been even more challenging.

Larger plot sizes could have been realized with a smaller sample size only. However it was decided to stick to a large sample size. This decision preserved the option to downsample the samples to larger plots as it was done in Lingner et al. (2018b).

Discussion of Results

Dry mass per SfM volume

Lingner et al. (2018c) estimated a slope of 1.79 $kg \cdot m^{-3}$ between volume and dry mass. However Lingner et al. (2018b) estimated a slope of 1.14 $kg \cdot m^{-3}$. The difference between these values is due to the difference in volume calculation. The volume in Lingner et al. (2018c) is modelled like a wrapping cloth. However the volume in Lingner et al. (2018b) is modelled based on pillars. Calculating the volume based on pillars turned out to be more reproducible and stable at point clouds with no points from the ground underneath the object. When generating an SfM model of a comparably wide object like a roadside planting there will be no or few 3D points from the ground underneath the object. At smaller objects like a hedge banks this problem is less pronounced since the ground is modelled better in smaller objects. Consequently this problem did not occur in Lingner et al. (2018c).

When calculating the volume based on pillars the volume under overhanging branches is included. Consequently the volume is a little higher compared to the other approach. This pattern leads to a different slope in the two methods.

Unfortunately no literature is published about this topic at the time of writing. So values could not be compared.

Growth per area and year

Lingner et al. (2018a) indicated that dry mass growth in linear forest objects is not linearly related to age but sigmoidally. Seidel et al. (2015) assumed a linear dry mass growth rate of 0.7 $kg \cdot m^{-2} \cdot a^{-1}$ in linear forest objects in central Germany where a is year and the area is the canopy area. This assumption could not be supported for northern Germany by the results of Lingner et al. (2018c). This study estimated a linear growth rate of 0.44 $kg \cdot m^{-2} \cdot a^{-1}$. Uckert (1998) has weighed multiple hedge banks in Schleswig-Holstein and calculated a growth rate of 0.5 $kg \cdot m^{-2} \cdot a^{-1}$. Walther and Bernath (2009) recommends a growth rate of 0.5 $kg \cdot m^{-2} \cdot a^{-1}$ as well. Apparently when assuming a linear growth rate at hedge banks this growth rate is rather around 0.5 $kg \cdot m^{-2} \cdot a^{-1}$ and not around 0.7 $kg \cdot m^{-2} \cdot a^{-1}$ for northern Germany. Consequently when estimating the dry mass of a linear forest object in Schleswig-Holstein a growth rate of 0.5 $kg \cdot m^{-2} \cdot a^{-1}$ should be preferred over a growth rate of 0.7 $kg \cdot m^{-2} \cdot a^{-1}$.

Further applications

The relationship between weight and volume appears to be similar in hedge banks and roadside plantings as presented in (Lingner et al., 2018b). This arises the question

whether this method is applicable to larger forest objects as well. The next larger step might be short rotation forestries. It was experienced that an undetailed enclosing SfM model of a short rotation forestry is possible with photos taken from a larger distance. However any detailed models are hard to generate due the similarity of the trees. The next larger step after short rotation forestries might be entire forests. The challenge with forests is that the ground level has to be guessed. At hedge banks and roadside plantings it is comparably easy to estimate the ground level. However at larger objects this might be difficult especially in a hilly landscape. Dandois and Ellis (2010) have already experienced that ground level estimation is challenging and faulty in larger forest objects when applying SfM. However their study shows promising results when applying Lidar for ground level estimation.

Future applications

The model generation for a linear forest object via UAV is time-consuming. It is likely that less time consuming methods are available in future. Google maps already presents 3D models of trees in some populated areas. However at the time of writing these data could not be accessed or processed. Another future approach could be the analysis of 3D satellite data. These data can be bought as digital surface models from service providers like AW3D. The disadvantage of these spaceborne digital surface models is the minimum purchase size of usually 25 km^2 and its high costs. These data usually can be bought with a vertical resolution of 0.5 m. This resolution should be sufficient for volume calculations of roadside plantings and hedge banks.

References

J. P. Dandois and E. C. Ellis. Remote Sensing of Vegetation Structure Using Computer Vision. *Remote Sensing*, 2(4):1157–1176, Apr. 2010. doi: 10.3390/rs2041157. URL http://www.mdpi.com/2072-4292/2/4/1157.

S. Dittmann, E. Thiessen, and E. Hartung. Applicability of different non-invasive methods for tree mass estimation: A review. *Forest Ecology and Management*, 398: 208–215, 2017.

J. Eigner. Bewertung von Knicks in Schleswig-Holstein. *Laufener Seminarbeitraege*, 5(82):110–117, 1982.

S. Lingner, E. Thiessen, and E. Hartung. Dry mass in linear forest objects: Sfm sensitivity, sfm vs. expert, growth pattern vs. age and vs. ecological value. *unpublished*, 2018a.

S. Lingner, E. Thiessen, and E. Hartung. Biomass estimation in linear forest objects: Structure from motion vs. aerial images. *unpublished*, 2018b.

S. Lingner, E. Thiessen, K. Müller, and E. Hartung. Dry Biomass Estimation of Hedge Banks: Allometric Equation vs. Structure from Motion via Unmanned Aerial Vehicle. *Journal of Forest Science*, 64(4):149–156, 2018c.

J. Miller, J. Morgenroth, and C. Gomez. 3d modelling of individual trees using a handheld camera: Accuracy of height, diameter and volume estimates. *Urban Forestry & Urban Greening*, 14(4):932–940, 2015. ISSN 16188667. doi: 10.1016/j.ufug.2015.09.001. URL http://linkinghub.elsevier.com/retrieve/pii/S1618866715001223.

D. Seidel, F. Beyer, D. Hertel, S. Fleck, and C. Leuschner. 3d-laser scanning: A non-destructive method for studying above- ground biomass and growth of juvenile trees. *Agricultural and Forest Meteorology*, 151(10):1305–1311, Oct. 2011a. ISSN 01681923. doi: 10.1016/j.agrformet.2011.05.013. URL http://linkinghub.elsevier.com/retrieve/pii/S0168192311001717.

D. Seidel, C. Leuschner, A. Müller, and B. Krause. Crown plasticity in mixed forests—quantifying asymmetry as a measure of competition using terrestrial laser scanning. *Forest Ecology and Management*, 261(11):2123 – 2132, 2011b. ISSN 0378-1127. doi: https://doi.org/10.1016/j.foreco.2011.03.008. URL http://www.sciencedirect.com/science/article/pii/S0378112711001514.

D. Seidel, S. Fleck, and C. Leuschner. Analyzing forest canopies with ground-based laser scanning: A comparison with hemispherical photography. *Agricultural and Forest Meteorology*, 154-155:1–8, Mar.

2012. ISSN 01681923. doi: 10.1016/j.agrformet.2011.10.006. URL http://linkinghub.elsevier.com/retrieve/pii/S0168192311003054.

D. Seidel, G. Busch, B. Krause, C. Bade, C. Fessel, and C. Kleinn. Quantification of Biomass Production Potentials from Trees Outside Forests – A Case Study from Central Germany. *BioEnergy Research*, 8(3):1344–1351, Sept. 2015. ISSN 1939-1234, 1939-1242. doi: 10.1007/s12155-015-9596-z.

N. Snavely, S. M. Seitz, and R. Szeliski. Modeling the World from Internet Photo Collections. *International Journal of Computer Vision*, 80(2):189–210, Dec. 2007. ISSN 0920-5691, 1573-1405. doi: 10.1007/s11263-007-0107-3.

D. Turner, A. Lucieer, and C. Watson. An Automated Technique for Generating Georectified Mosaics from Ultra-High Resolution Unmanned Aerial Vehicle (UAV) Imagery, Based on Structure from Motion (SfM) Point Clouds. *Remote Sensing*, 4(12):1392–1410, May 2012. ISSN 2072-4292. doi: 10.3390/rs4051392. URL http://www.mdpi.com/2072-4292/4/5/1392/.

G. B. Uckert. Art- und raumspezifische ermittlung der biomasseproduktion von knicks in schleswig-holstein. Master's thesis, Christian-Albrechts-Universität Kiel, 1998.

R. Walther and K. Bernath. *Energieholzpotenziale ausserhalb des Waldes. Studie im Auftrag des Bundesamtes für Umwelt (BAFU) und des Bundesamtes für Energie (BFE).* Ernst Basler + Partner, 2009.

7 Summary

Summary

According to the European Renewable Energy Directive (2009/28/EG) renewable energy is supposed to cover at least 20 % of the gross energy consumption in 2020 within the European Union. In Germany, the amount of woody biomass used as a source for energy has already increased during the last decades. The future demand for woody biomass could in part be supplied by harvested wood of existing hedge banks and roadside plantings. The aim of the current thesis was to develop and to test a technique for biomass estimation at linear forest objects. At first the literature was searched for different methods of woody biomass estimation. At second different methods were tested at linear forest objects in Schleswig-Holstein and the results were compared to reference dry masses.

Chapter 2 presents the literature review of biomass estimation techniques at various different spatial scales. The conclusion of this chapter is: Allometric approaches are comparably accurate, but time consuming. Consequently, they are suitable for small area applications only. Lidar and structure from motion (SfM) appear to be the most efficient and most accurate techniques for medium sized area applications. Especially SfM applications are promising due to lower technical requirements. Optical images are suitable for coarse but large area applications. In summary allometric approaches, SfM approaches and approaches based on optical images are worth to be tested for linear forest objects.

Chapter 3 compares two methods of wood yield estimation at hedge banks. Test objects were three hedge banks in Schleswig-Holstein. The first method was an estimation based on allometric equation via diameter at breast height (DBH) and achieved an relative root mean square error (rRMSE) of 32 %. The second method was an estimation based on SfM and resulted in an rRMSE of 30 %. These results showed that SfM approaches are reasonably precise but are a lot less time consuming than approaches based on allometric equations. Consequently SfM applications appear to be the better approach for biomass estimations at hedge banks.

Chapter 4 compares two methods of wood yield estimation at eleven linear forest objects. Test objects were five hedge banks and six roadside plantings in Schleswig-Holstein. The first method was an estimation based on aerial images plus age of object and achieved an rRMSE of 52 %. Like in Chapter 3 the second method was an estimation based on SfM and resulted in an rRMSE of 30 %. These results showed that SfM approaches are notably more accurate than predictions based on area and age. Consequently SfM applications again appear to be the better approach for biomass estimations at linear forest objects.

Chapter 5 addressed multiple questions that arose during the process of the previous papers. The topics investigated further in this chapter were: Analysis of sensitivity (seasonal effect, amount of images, resolution of images), SfM vs. experienced person,

temporal pattern of growth and growth pattern vs. ecological value. The results showed the following: Images for SfM models can be taken both in summer or autumn. A resolution of 6 megapixels is sufficient for SfM applications at trees. Consequently a consumer UAV is good enough. The predictions by the SfM models were comparable to the predictions by experts, but need less experience. The dry mass growth rate in linear forest objects is not linear but sigmoidal. Consequently to maximize yield the objects should not be harvested before 25 years of growth. Dry mass yield per area and age did not depend on the the ecological value. In conclusion there is no reason not to support a species composition with a high ecological value.

The general discussion covers experiences gained, decisions made and recommendations for the future that are worth to be discussed generally for all previous chapters.

Zusammenfassung

Gemäß der Erneuerbare-Energien-Richtlinie (2009/28/EG) soll der Anteil von erneuerbaren Energien am Gesamtenergieverbrauch im Jahr 2020 innerhalb der Europäischen Union bei mindestens 20 % liegen. In Deutschland hat die Menge des zur Energiegewinnung genutzten Holzes bereits in den letzten Jahrzehnten deutlich zugenommen. Der zukünftige Bedarf an Holz kann zum Teil aus existierenden Knicks und Straßenbegleitgrünen gewonnen werden.

Das Ziel dieser Arbeit war es, eine Methode zu entwickeln, um in solchen linearen Forstobjekten die Holzmasse abzuschätzen. Zunächst wurde die Literatur nach verschiedenen Methoden der Holzmassenabschätzung durchsucht. Anschließend wurden verschiedene dieser Methoden an linearen Forstobjekten in Schleswig-Holstein getestet. Die Ergebnisse der Schätzungen wurden mit gewogenen Holzmassen verglichen.

Chapter 2 präsentiert die Literaturrecherche zur Biomasseabschätzung an Bäumen auf verschiedenen räumlichen Skalen. Das Ergebnis dieses Kapitels ist: Allometrische Gleichungen sind vergleichsweise genau, allerdings auch sehr zeitintensiv. Daher lassen sie sich nur kleinräumig anwenden. Lidar und Structure from Motion (SfM) erschienen die effizientesten und die genauesten Anwendungen für mittelgroße Flächen zu sein. Insbesondere SfM erscheint vielversprechend, da es geringe technische Anforderungen hat. Die Auswertungen von Luftbilden hingegen eignet sich für großflächige und grobe Vorhersagen. Insgesamt bieten sich allometrische Gleichungen, SfM-Anwendungen und Anwendungen basierend auf Luftbilden an, um sie bezüglich ihrer Vorhersagekraft bei linearen Forstobjekten zu testen.

Chapter 3 vergleicht zwei Methoden der Holzabschätzung an Knicks. Die Testobjekte waren drei Knicks in Schleswig-Holstein. Die erste Methode basierte auf allometrischen Gleichungen auf Grundlage des Brusthöhendurchmessers und erreichte einen rRMSE von 32 %. Die zweite Methode basierte auf SfM und erreichte einen rRMSE von 30 %. Die Ergebnisse zeigen, dass die Vorhersagekraft von SfM-Anwendungen vergleichbar mit der aus allometrischen Gleichungen ist. Jedoch ist SfM deutlich weniger zeitintensiv als die Datenaufnahme für allometrische Gleichungen. Folglich erscheinen SfM-Anwendungen besser geeignet zu sein, um Biomasse in Knicks abzuschätzen.

Chapter 4 vergleicht zwei Methoden der Holzabschätzung an elf linearen Forstobjekten. Die Testobjekte waren fünf Knicks und sechs Straßenbegleitgrüne in Schleswig-Holstein. Die erste Methode war eine Abschätzung basierend auf Luftbildern und des Alters der Objekte und erreichte einen rRMSE von 52 %. Wie in Chapter 3 war die zweite Methode eine Abschätzung basierend auf SfM und erreichte einen rRMSE von 30 %. Die Ergebnisse zeigen, dass die Vorhersagen der SfM-Methode deutlich genauer sind als die Abschätzungen über Luftbilder und das Alter. Folglich erscheinen SfM-Anwendungen erneut besser geeignet zu sein, um Biomasse in linearen Forstobjekten abzuschätzen.

Chapter 5 behandelt einige Fragen, welche während des Forschungsprozesses entstanden sind. Die Themen welche hier weiter untersucht wurden sind: Sensitivitätsanalyse (saisonale Effekte, Anzahl benötigter Bilder, benötigte Auflösung), SfM gegenüber Expertenschätzung, der Zuwachs in Abhängigkeit zur Zeit und der Zuwachs in Abhängigkeit zum ökologischen Wert. Die Ergebnisse zeigten folgendes: Bilder für

SfM-Anwendungen können sowohl im Sommer als auch im Herbst aufgenommen werden. Eine Auflösung von 6 Megapixeln ist ausreichend für SfM-Anwendungen bei Bäumen. Folglich reicht die Auflösung einer handelsüblichen Drohne. Die Vorhersagekraft von SfM-Modellen war vergleichbar mit den Vorhersagen von Experten, jedoch benötigen SfM-Modelle weniger Erfahrung. Die Wuchsrate von linearen Forstobjekten zeigte sich nicht linear, sondern sigmoidal. Die Objekte sollten nicht vor 25 Jahren geerntet werden, um einen maximalen Ertrag zu erhalten. Der Ertrag pro Jahr und Fläche war nicht abhängig von der ökologischen Wertigkeit. Folglich gibt es keinen Grund auf eine hohe ökologische Wertigkeit in den Objekten zu verzichten.

Die Diskussion beinhaltet gesammelte Erfahrungen, getroffene Entscheidungen und Empfehlungen für die Zukunft, welche es wert sind, zusammenfassend über alle Kapitel diskutiert zu werden.

Declaration of co-authorship

If a dissertation is based on already published or submitted co-authored articles, a declaration from each of the authors regarding the part of the work done by the doctoral candidate must be enclosed when submitting the dissertation.

1. Doctoral candidate
Stefan Lingner

2. This co-author declaration applies to the following article:
Applicability of different non-invasive methods for tree mass estimation: a review

The extent of the doctoral candidate's contribution to the article is assessed on the following scale:

A. Has contributed to the work (0-33%)
B. Has made a substantial contribution (34-66%)
C. Did the majority of the work independently (67-100%)

3. Declaration on the individual phases of the scientific work (A,B,C)	Extent
Stefan Lingner	C
Eiko Thiessen	A
Eberhard Hartung	A

4. Signature of all co-authors		
Lingner		16.11.18
Thiessen		16.11.18
Hartung		23/11/18

5. Signature of doctoral candidate		
Lingner		16.11.18

C | A | U	Christian-Albrechts-Universität zu Kiel	Agrar- und Ernährungs-wissenschaftliche Fakultät

Declaration of co-authorship

If a dissertation is based on already published or submitted co-authored articles, a declaration from each of the authors regarding the part of the work done by the doctoral candidate must be enclosed when submitting the dissertation.

1. Doctoral candidate
Stefan Lingner

2. This co-author declaration applies to the following article:
Dry biomass estimation of hedge banks: Allometric equation vs. Structure from Motion via Unmanned Aerial Vehicle

The extent of the doctoral candidate's contribution to the article is assessed on the following scale:

A. Has contributed to the work (0-33%)
B. Has made a substantial contribution (34-66%)
C. Did the majority of the work independently (67-100%)

3. Declaration on the individual phases of the scientific work (A,B,C)	Extent
Stefan Lingner	C
Eiko Thiessen	A
Kerrin Müller	A
Eberhard Hartung	A

4. Signature of all co-authors		
Lingner		16.10.'18
Thiessen		16.10.'18
Müller	K. Bujonsonja geb. Müller	24.10.2018
Hartung		22/11/18

5. Signature of doctoral candidate		
Lingner		16.11.'18

Declaration of co-authorship

If a dissertation is based on already published or submitted co-authored articles, a declaration from each of the authors regarding the part of the work done by the doctoral candidate must be enclosed when submitting the dissertation.

1. Doctoral candidate
Stefan Lingner

2. This co-author declaration applies to the following article:
Biomass estimation in linear forest objects: Structure from Motion vs. aerial images

The extent of the doctoral candidate's contribution to the article is assessed on the following scale:

A. Has contributed to the work (0-33%)
B. Has made a substantial contribution (34-66%)
C. Did the majority of the work independently (67-100%)

3. Declaration on the individual phases of the scientific work (A,B,C)	Extent
Stefan Lingner	C
Eiko Thiessen	A
Eberhard Hartung	A

4. Signature of all co-authors		
Lingner		16.11.18
Thiessen		16.11.18
Hartung		23/11/18

5. Signature of doctoral candidate		
Lingner		16.11.18

C | A | U Christian-Albrechts-Universität zu Kiel | Agrar- und Ernährungswissenschaftliche Fakultät

Declaration of co-authorship

If a dissertation is based on already published or submitted co-authored articles, a declaration from each of the authors regarding the part of the work done by the doctoral candidate must be enclosed when submitting the dissertation.

1. Doctoral candidate
Stefan Lingner

2. This co-author declaration applies to the following article:
Dry mass in linear forest objects: Structure from Motion sensitivity, Structure from Motion vs. expert, temporal pattern of growth and growth pattern vs. ecological value

The extent of the doctoral candidate's contribution to the article is assessed on the following scale:

A. Has contributed to the work (0-33%)
B. Has made a substantial contribution (34-66%)
C. Did the majority of the work independently (67-100%)

3. Declaration on the individual phases of the scientific work (A,B,C)	Extent
Stefan Lingner	C
Eiko Thiessen	A
Eberhard Hartung	A

4. Signature of all co-authors		
Lingner		16.11.18
Thiessen		16.11.18
Hartung		23/11/18

5. Signature of doctoral candidate		
Lingner		16.11.18